Article

Current Biology

Contrasting population structures of reef-building corals and their algal symbionts inform adaptive potential across the western Pacific

Highlights

- Western Pacific corals and their algal symbionts show distinct genetic structure
- Large coral populations and widespread dispersal support demographic resilience
- Habitat-specific symbioses and gene flow across regions may underpin adaptation
- Management of coral populations as interconnected units supports ongoing adaptation

Authors

Hugo Denis, Katharine E. Prata, Hisatake Ishida, ..., Cynthia Riginos, Emily J. Howells, Véronique Berteaux-Lecellier

Correspondence

denis.hugo08@gmail.com

In brief

Using extensive geographic sampling and hologenome data, Denis et al. uncover distinct eco-evolutionary processes shaping genetic connectivity and diversity in a reef-building coral and its associated algal symbionts. These processes influence demographic resilience and evolutionary adaptation, underscoring their importance for management interventions and conservation networks that extend beyond national borders.

Denis et al., 2026, Current Biology *36*, 2808–2822
June 8, 2026
https://doi.org/10.1016/j.cub.2026.04.057

CellPress

CellPress
OPEN ACCESS

Current Biology

Article

Contrasting population structures of reef-building corals and their algal symbionts inform adaptive potential across the western Pacific

Hugo Denis,[1,2,3,10,*] Katharine E. Prata,[4,5] Hisatake Ishida,[6] Iva Popovic,[4,5] Véronique J.L. Mocellin,[4] Magali Boussion,[1] Ilha Byrne,[5] Steven W. Purcell,[3] Line K. Bay,[4] Gaël Lecellier,[7] Cheong Xin Chan,[6] Cynthia Riginos,[4,5] Emily J. Howells,[3,8,9] and Véronique Berteaux-Lecellier[1,9]

[1]Santé des Ecosystèmes Tropicaux (SantEco) EMR9001, CNRS, IRD, Université de Nouvelle-Calédonie, Université la Reunion, UMR 250 ENTROPIE, Noumea 98800, New Caledonia, France
[2]ED 129, SU Sorbonne Université, 4, Place Jussieu, Paris 75252, France
[3]National Marine Science Centre, Faculty of Science and Engineering, Southern Cross University, Coffs Harbour, NSW 2450, Australia
[4]Australian Institute of Marine Science, Townsville, QLD 4810, Australia
[5]School of the Environment, University of Queensland, Brisbane, QLD 4072, Australia
[6]Australian Centre for Ecogenomics, School of Chemistry and Molecular Biosciences, University of Queensland, Brisbane, QLD 4072, Australia
[7]Institut de Sciences Exactes et Appliquées (ISEA) EA7484, 145, Avenue James Cook, BP R4, 98 851 Nouméa, New Caledonia, France
[8]Lizard Island Research Station, Australian Museum, Sydney, NSW 2010, Australia
[9]These authors contributed equally
[10]Lead contact
*Correspondence: denis.hugo08@gmail.com
https://doi.org/10.1016/j.cub.2026.04.057

SUMMARY

The genetic diversity and connectivity of reef-building coral populations are key to their survival in warming oceans. Yet our understanding of corals' demographic resilience and adaptive potential is complicated by cryptic species diversity, wide geographic distributions, and complex coral-algal symbioses. To address these challenges, we investigated the genetic connectivity and diversity of the broadcast-spawning coral *Acropora* cf. *spathulata* and its associated Symbiodiniaceae across 29 reefs spanning the Great Barrier Reef, the Coral Sea, and New Caledonia, using whole-genome sequencing of 1,088 colonies. We identified four genetically distinct coral populations that diverged between 0.27 and 0.65 mya, likely due to geographic isolation across thousands of kilometers. These populations maintained asymmetrical gene flow along major ocean currents despite demographic isolation and sustained large local effective population sizes (~2,900), supported by a high dispersal range of ~100 km per generation. In contrast, their Symbiodiniaceae partners varied over finer spatial scales, with five distinct *Cladocopium* taxa distributed along latitudinal and cross-shore gradients, likely driven by local environmental conditions. These results suggest that high dispersal capacity and large local population size promote demographic resilience within reef systems, while environment-specific symbioses and long-distance gene flow across reef systems support adaptation and evolutionary rescue.

INTRODUCTION

Reef-building corals and their microbial symbionts constitute coral holobionts that are the foundation of biodiverse but threatened coral reef ecosystems.[1] As tropical corals are declining globally, it is crucial to better understand the evolutionary, spatial, and environmental processes that shape their population dynamics and resilience.[2,3] However, the widespread presence of cryptic coral diversity[4,5] and taxonomically overlooked species,[6,7] along with vast geographic ranges,[8] challenges our ability to determine the size and connectivity of coral populations. In addition, variability in symbioses between coral hosts and symbiotic microalgae from the family Symbiodiniaceae can affect holobionts' capacity to grow, survive, and adapt under changing conditions.[9]

Population genomics, which investigates genome-wide molecular variation, can differentiate coral taxa that are indistinguishable based on morphological criteria[10] or traditional population genetic markers such as microsatellites.[11,12] Within coral species, population genomics can provide a holistic view of spatial genetic variation patterns in both hosts and symbionts across their range.[13] These analyses are essential for uncovering the distinct scales at which gene flow, local adaptation, and co-evolutionary dynamics influence the adaptive responses of holobionts.

Contemporary gene flow (over tens of generations) is crucial for coral demographic dynamics, particularly for the recovery of locally depleted coral populations following perturbations.[14,15] To quantify its spatial extent, the isolation-by-distance (IbD)

theory provides a useful framework by estimating a generational gene dispersal distance.[16,17] Combining the slope of IbD with estimates of effective density, one can infer the generational mean axial dispersal distance (σ), over which most dispersal events occur, and vast differences in σ depending on reproductive modes and taxa have been described.[18–21] To estimate effective density, the local effective population size (N_e) is estimated and divided by the area the population occupies. Local N_e indicates the loss rate of genetic variation due to genetic drift at the scale where most breeding events occur.[22] This standing variation, on which natural selection acts, underpins adaptive potential.[23] Jointly estimating σ and N_e thus provides crucial information on the extinction risk of local coral populations[24] and the spatial scale of demographic replenishment,[25] both of which are essential for defining conservation units.

Over longer evolutionary timescales, occasional long-distance dispersal can affect species range and adaptation to global change.[26] However, methods based on high-level genetic differentiation cannot disentangle the effect of migration from genetic drift and shared ancestry or determine the direction of gene flow.[27,28] Demographic history inference approaches that model divergence times, variation in migration rates, and long-term effective population sizes[29] offer a complementary strategy to assess gene flow across a coral species range.[18] However, despite potential for coral connectivity spanning thousands of kilometers,[30,31] such methods have been primarily applied within national borders.[18,30,32,33] This limits the development of coordinated regional conservation strategies that incorporate gene flow from different regions to assess the evolutionary adaptation potential of corals.[34]

Importantly, coral evolution and conservation require consideration of their symbiosis with Symbiodiniaceae microalgae[35] that are genetically and physiologically diverse.[36] For instance, the photosynthetic ability of Symbiodiniacae is known to differ among taxa under heat stress[37]; some taxa inhabit warmer environments[38] or increase in prevalence during thermal stress.[39] Most Symbiodiniaceae are facultative symbionts; therefore, both macro-environments and host micro-environments will favor certain taxa or genotypes.[40–42] In turn, some symbiont taxa may facilitate corals' local adaptation to environmental conditions.[43] Symbiont diversity has been mostly described using phylogenetic markers such as the ribosomal internal transcribed spacer 2 (ITS2)[44] and the chloroplastic non-coding region of the *psbA* gene, i.e., psbA^{ncr},[45] or via multilocus genotyping (e.g., Davies et al.[46] and Lewis et al.[47]). Yet distinguishing intra- from inter-genomic variants remains challenging, and the dependence on a few selected marker genes may limit taxonomic resolution.[48] Emerging methods based on genome-wide sequence composition of hologenome samples,[32,49] or the recovery of additional mitochondrial and chloroplast markers from these samples,[32,48–50] are uncovering previously hidden phylogenetic and ecological diversity.

Acropora cf. *spathulata* is a fast-growing, broadcast spawning, and widespread species that inhabits shallow reef environments in the western Pacific, including the Great Barrier Reef (GBR), the Coral Sea, and New Caledonia (NC). Genetic data have revealed new insights into the cryptic diversity of *Acropora* corals on the GBR, including lineages that are morphologically indistinguishable or previously overlooked,[51,52] their associated Symbiodiniaceae[51–54] and realized connectivity, dominated by southward migration of coral larvae.[30,55] However, such information remains scarce in NC, with only one genomic study conducted to date on *Acropora* coral hosts[56] and few on their symbiont communities.[57–59] In addition, despite being one of the most studied coral reef ecosystems,[60] the GBR's connectivity with nearby western Pacific Islands such as NC remains unknown. Several ocean currents flow westward and eastward between the GBR and NC (Figure S1A),[61] offering potential for periodical dispersal via stepping-stone migration through Coral Sea atolls, e.g., the Chesterfield-Bellona (CB) plateau. To our knowledge, no study in corals has systematically assessed gene flow in this western Pacific region, aside from pumice-rafting coral larvae from NC to the GBR,[62] and some genetic admixture between these reef systems and Coral Sea atolls.[63–65] NC and the southern GBR are often considered potential climate refugia with projected stability of coral cover[66,67] due to the mild occurrence of bleaching until recently.[68] Understanding whether these systems have or still exchange migrants is therefore important for their regional conservation.

Here, we systematically assess the host and symbiont population structures and gene flow of the coral *Acropora* cf. *spathulata*, expanding the common research scope of the GBR[50,51,69–71] to the western Pacific. By integrating existing and innovative genome-scale approaches, we densely sampled, sequenced, and analyzed whole-genome sequencing data from 1,088 colonies from 29 reefs across the GBR, the Coral Sea, and NC. Our study represents one of the most geographically comprehensive efforts to concurrently investigate coral host and symbiont diversity, as well as contemporary and long-term connectivity.

RESULTS

Genomic data processing and filtering

We recovered 339,720 single-nucleotide polymorphisms (SNPs) from 1,088 individual coral colonies of *Acropora* cf. *spathulata*, using a stringent filtering approach (STAR Methods; Tables S1–S3). This dataset had a mean locus-level sequencing depth of 13.7 ± 1.2 (mean ± SD). Following removal of related individuals and linked SNPs, dataset 1, used for population structure analyses, comprised 999 individuals and 27,175 SNPs (Table S4). Dataset 2, used to compute genetic differentiation and diversity metrics, consisted of ~2.2 M loci (SNPs and monomorphic sites). Dataset 3, used for demographic modeling, consisted of 37,841–61,902 SNPs per population pair, and dataset 4, used for IbD analyses and N_e estimates, consisted of 2,011 SNPs after pruning for physical linkage (Table S4).

Coral host population structure

A. cf. *spathulata* colonies across the western Pacific were separated into four genetically differentiated groups, hereinafter referred to as populations (Figure 1). A principal-component analysis (PCA) revealed geographically distinct populations separated on PC1 and PC2 (1.5% and 0.7% explained variance, respectively; Figure 1A), corresponding to the central to northern GBR (i.e., from Davies to Hicks reefs), the southern GBR, the CB atolls in the Coral Sea, and the west coast of the main island of NC. PC3 (0.5% explained variance; Figure 1A) separated the

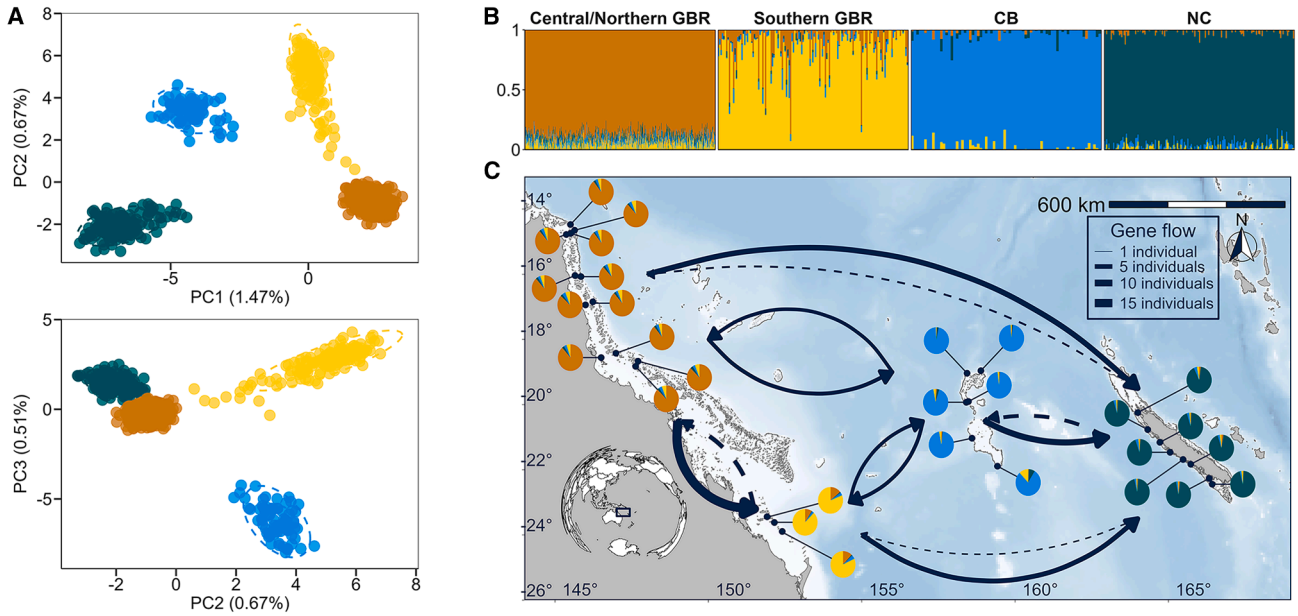

Figure 1. Population genomic structure and connectivity of *Acropora* cf. *spathulata* across reefs from the GBR, CB atolls, and NC

(A) PCA based on 27,175 SNPs showing four genetically and geographically distinct populations across the western Pacific. PC1, PC2, and PC3 are shown with the proportion of variance explained by each component indicated in percentages.

(B) Ancestry proportions from each individual using ADMIXTURE analysis with the optimal number of ancestral populations found using cross-validation ($K = 4$).

(C) Map showing ancestry proportion at sampling sites, averaged across colonies ($n = 4$–60). Arrows indicate average gene flow, in number of migrants per generation, between populations since their divergence, inferred from demographic modeling in ∂a∂i. Solid and dashed lines indicate the primary and secondary directions of gene flow, respectively. Solid lines are shown in both directions when confidence intervals overlap.

See also Figures S2–S4.

CB group from the three other groups. Similarly, ADMIXTURE and sparse non-negative matrix factorization (sNMF) analyses identified a concordant optimal number of $K = 4$ ancestral populations (Figures 1 and S2A–S2D). The separation of individuals by their ancestry proportion was consistent with PCA results but revealed low levels of admixture between all populations (Figure 1B). In particular, 4 of 137 and 19 of 137 colonies from the southern GBR had >0.5 and >0.25 assignments to the ancestral population of the central/northern GBR, respectively. Additional ADMIXTURE analyses conducted within each major population revealed no evidence of finer-scale population structure among reefs (Figures S3A–S3D).

Population divergence and genetic diversity

Genetic divergence, estimated using the fixation index, was low between all four populations ($F_{st} < 0.030$; Table 1) and was lowest between the two GBR populations ($F_{st} = 0.014$). Pairwise D_{xy} ranged from 0.010 to 0.011 and was lowest between the NC and CB populations. This corresponds to an average 1% nucleotide difference per base pair between populations (Table 1). Nucleotide diversity (π) was highest in the NC population ($\pi = 0.0106$), followed by the central/northern GBR ($\pi = 0.0103$) and the southern GBR populations ($\pi = 0.0100$). The CB population had the lowest nucleotide diversity ($\pi = 0.0097$).

Dispersal and effective population size

No significant IbD occurred within populations. However, the pattern of IbD was revealed when populations were analyzed jointly, with the regression of individual Rousset's genetic distance on geographic distance yielding a significant positive slope ($\beta = 0.00064 \pm 3.7 \times 10^{-5}$; median ± SD; Figure 2A). The effective population size at the neighborhood size across this geographic range was estimated at $N_e = 2{,}954 \pm 1{,}573$ effective individuals (median ± SD; Figure 2B). Combining these estimates, the average dispersal distance between parents and offspring across generations was 109 ± 33 km (mean axial dispersal distance; σ; median ± SD; Figure 2C).

Demographic modeling of population divergence and gene flow

For all population pairs, observed joint allelic frequency spectra (JAFS) were better explained by demographic models consisting of divergence with asymmetrical gene flow than models with no gene flow or only ancestral gene flow (Figure S4). This suggests that these populations have diverged across the western Pacific while exchanging larvae over many generations. Demographic models estimated divergence time between 275 and 651 thousand years ago (kya), depending on population pairs (Table 1), although these are approximate estimates because germline mutation rates are lacking for this species. Based on these estimates, the two populations from the GBR appear to have diverged most recently (275 [230–319] kya; median [5%–95%]). Modeling results suggest that divergence of NC from other populations (323–651 kya) is more ancient than that of CB from GBR populations (354–385 kya). However, large overlaps in confidence intervals and possible bias introduced by high migration rates make it difficult to reconstruct their precise sequential divergence history.

Table 1. Demographic modeling of *Acropora* cf. *spathulata* population divergence across the western Pacific

	Effective population size			Proportion of migrants per generation		Number of migrants per generation		Divergence time	Genetic differentiation	
Population pair	Ancestral Nref	Current ν_1	Current ν_2	m_{12} (2 → 1)	m_{21} (1 → 2)	M_{12} ($N_e m_{12}$)	M_{21} ($N_e m_{21}$)	T	D_{XY}	F_{st}
1 central/northern GBR; **2** southern GBR	**7.2** [4.1, 10.6]	**63.9** [51.1, 76.3]	**32.5** [25.9, 42.3]	**6.2e–5** [4.6e–5, 8.7e–5]	**2.5e–4** [2.0e–4, 3.0e–4]	**7.9** [6.6, 9.6]	**16.4** [14.7, 18.0]	**276** [231, 320]	0.0102	0.014
1 central/northern GBR; **2** New Caledonia	**9.2** [5.1, 17.6]	**82.9** [66.9, 118.9]	**25.0** [14.5, 33.6]	**2.1e–5** [9.4e–6, 3.5e–5]	2.0e–4 [1.5e–4, 3.0e–4]	**3.6** [2.3, 4.7]	**9.9** [8.6, 11.0]	**323** [218, 379]	0.0107	0.025
1 central/northern GBR; **2** Chesterfields-Bellona	**4.9** [3.7, 9.9]	**61.9** [51.1, 75.8]	**29.6** [21.6, 36.6]	**5.4e–5** [3.7e–5, 7.2e–5]	**1.2e–4** [9.2e–5, 1.7e–4]	**6.5** [5.2, 8.0]	**7.1** [6.5, 7.8]	**354** [292, 373]	0.0102	0.028
1 southern GBR; **2** New Caledonia	**6.5** [4.6, 10.9]	**82.0** [73.6, 87.9]	**32.8** [28.4, 39.5]	**1.7e–5** [1.3e–5, 2.5e–5]	**1.4e–4** [1.2e–4, 1.5e–4]	**2.8** [2.2, 3.7]	**8.8** [8.2, 9.5]	**436** [378, 461]	0.0107	0.029
1 southern GBR; **2** Chesterfields-Bellona	**7.1** [4.4, 12.3]	**65.8** [58.1, 74.5]	**34.8** [28.6, 43.9]	**5.1e–5** [3.5e–5, 7.1e–5]	**9.3e–5** [5.9e–5, 1.2e–4]	**6.8** [5.1, 8.6]	**6.3** [5.1, 7.3]	**395** [334, 431]	0.0100	0.026
1 New Caledonia; **2** Chesterfields-Bellona	**7.2** [6.6, 9.9]	**86.5** [76.4, 96.7]	**48.8** [35.2, 56.1]	**6.5e–5** [5.2e–5, 7.3e–5]	**7.0e–5** [5.6e–5, 1.1e–4]	**11.0** [9.8, 12.1]	**6.9** [6.2, 7.8]	**651** [630, 666]	0.0104	0.026

For each pair of populations, optimized parameters are presented for the model exhibiting the best fit to the observed joint allelic frequency spectrum (divergence with asymmetrical gene flow). N_{ref}, ν_1, and ν_2 are the ancestral and current effective population sizes in thousands of individuals (Figure S4A). *m* is the proportion of migrants per generation and *M* is the number of migrants per generation. *T* is the estimated divergence time in thousands of years. For each model and parameter, median (bold) and 2.5%–97.5% confidence intervals based on 100 optimized bootstrap replicates are presented. Genetic differentiation statistics are shown for each pair of populations (fixation index F_{st} and absolute divergence D_{xy}).See also Figure S4.

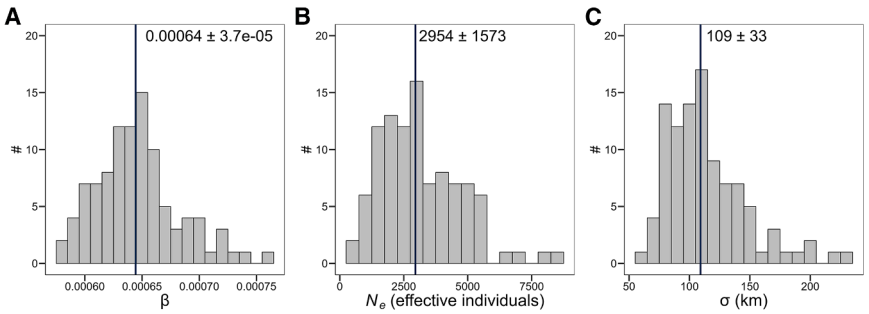

Figure 2. Generational dispersal and effective population size in *Acropora* cf. *spathulata* from the western Pacific

Isolation by distance at multiple appropriate spatial scales was used to infer the distribution of (A) slope of genetic distance on geographic distance regressions, (B) effective population size at the neighborhood scale, and (C) mean axial generational dispersal distance. Vertical lines indicate the median of each distribution, with median and standard deviation values indicated next to it.

Migration rates and gene flow rates were asymmetrical for most population pairs, and this result was consistent across bootstrap replicates and optimization runs (Table 1). On the GBR, migration rates were, on average, 5 times higher from the central/northern population to the southern population (2.5×10^{-4}) than vice versa (6.2×10^{-5}), resulting in higher southward gene flow (N_em), in line with predominant oceanographic currents (Figures 1C and S1A). Eastward migration rates from both GBR populations to the CB population (9.3×10^{-5}–1.2×10^{-4}) were higher than the westward rates (5.4×10^{-5}–1.2×10^{-4}). However, differences in long-term effective population sizes (29,000–66,000 effective individuals) resulted in nearly symmetrical gene flow between the GBR and these Coral Sea atolls (6.5–7.1 migrants per generation, Figure 1C). Migration rates between the CB and NC populations were broadly symmetrical ($6.5–7.0 \times 10^{-5}$), but the compounding effect of unequal population sizes produced a predominance of eastward gene flow (11.0 [9.8–12.1] migrants per generation; median [5%–95%]). Gene flow was also directed primarily eastward, from both GBR populations toward NC (Figure 1C).

Symbiodiniaceae genetic diversity based on molecular markers

We mapped non-coral reads from our 1,088 hologenomes to Symbiodiniaceae reference genomes and recovered a median of 708,000 Symbiodiniaceae reads per sample (range: 63,540–24,932,887). All colonies harbored symbionts from the *Cladocopium* genus, with predominant ITS2 sequence variants (recovered from hologenome reads in 950 of 1,088 samples) classified as C50, C3, and *Cladocopium* sp. (Figure S5A). Hologenome sequencing results were consistent with amplicon sequencing results in a subset of 36 samples, although the latter showed greater taxonomic resolution, separating profiles dominated by C3k, C3k/C3bo, C50b, and C50c sequences (Figure S6A). Read mapping against *psbA*^{ncr} sequences revealed classifications of *C. vulgare* (C1) or *C. sodalum* (C3; Figure S5A). The mapping of reads to *psbA*^{ncr} C1 in samples associated with C50 ITS2 sequences was presumably due to the lack of reference *psbA*^{ncr} sequences for *Cladocopium* C50, limiting the use of this method for finer taxonomic classification. However, our results suggest that the C3 symbionts identified are more closely related to *C. sodalum* than other described C3 species (>80% of mapped sequences).[72]

Symbiodiniaceae community divergence based on k-mer profiles

Alignment-free clustering of symbiont genomic reads revealed five major Symbiodiniaceae genetic clusters across colonies (Figures S5B and S5C), hereinafter referred to as taxa and named according to their major ITS2 sequence (Figure S6). There was some degree of co-clustering between each of the five main symbiont taxa and the corresponding host populations (Figure 3). The host population in the central/northern GBR was

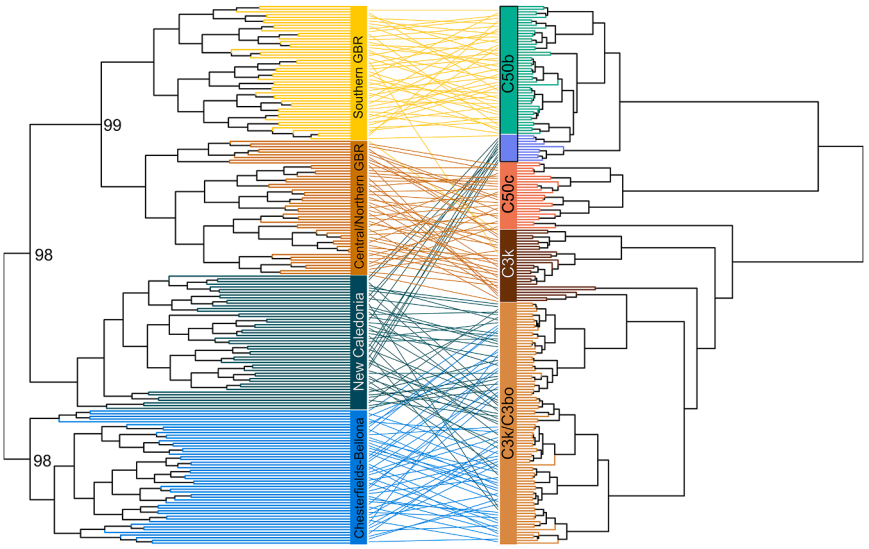

Figure 3. Co-clustering of *Acropora* cf. *spathulata* coral hosts and associated Symbiodiniaceae taxa across the western Pacific

The host dendrogram (left) is a simplified 200-leaf maximum-likelihood tree derived from 27,175 SNPs using RAxML. The node values represent bootstrap support (>90) from 100 bootstrap replicates and branches are colored based on ADMIXTURE ancestral populations (Figure 1). The symbiont dendrogram (right) is obtained through hierarchical clustering of the D_2^S-derived distance matrix based on symbiont *k*-mer profiles, and branches are colored according to majority ITS2 sequences for each sample (a complete NJ-tree for all samples can be found in Figure S5A). Colonies from the southern Great Barrier Reef (GBR) and NC were associated with Symbiodiniaceae that shared the same dominant ITS2 sequence (C50b; black rectangle) but were distinguishable based on their *k*-mer profiles (Figure S5C).
See also Figures S5 and S6.

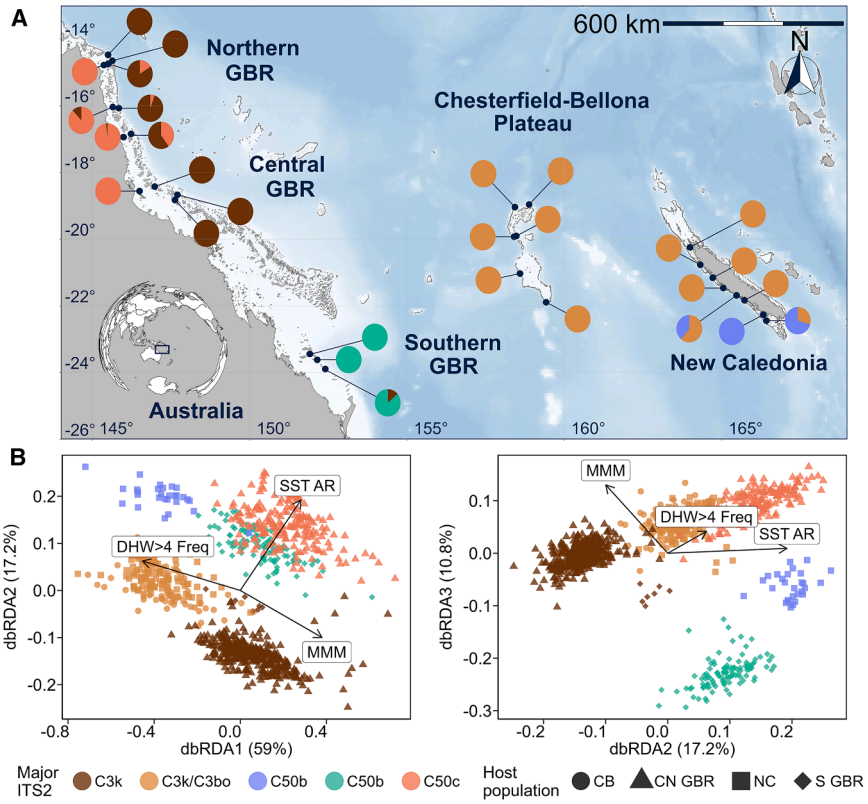

Figure 4. Variation in the symbiont (Symbiodiniaceae) communities of *Acropora* cf. *spathulata* across geographic and environmental gradients in the western Pacific

(A) Map showing the proportion of colonies harboring each of the symbiont clusters at each sampling site, identified using ordination of D_2^S distance matrix (Figures S5B and S5C). Symbiont genetic clusters are colored and labeled based on their major ITS2 type (Figure S6). Symbionts with the same dominant C50b ITS2 sequence are depicted with different colors in the southern GBR and NC, as they were found to be genetically differentiated based on their *k*-mer profiles (Figure S5C).

(B) Distance-based redundancy analysis (dbRDA) ordination of D_2^S *k*-mer profiles. Each individual is colored by its major ITS2 sequence and the shape corresponds to each of the host populations (CN GBR, central/northern GBR; S GBR, southern GBR; NC, New Caledonia; CB, Chesterfield-Bellona). Arrows represent significant environmental variables in the model. The first three axes explaining 87% of the constrained variance are shown.

See also Figure S1 and Table S5.

associated predominantly with *Cladocopium* taxa from C3k and C50c subclades, with a cross-shore partitioning of these communities. Offshore reefs were associated with C3k, while inshore reefs were associated with C50c (Figure 4A). At intermediate reefs (e.g., Moore, North Direction, and Mackay), some colonies harbored the C50c taxon while others harbored C3k. The host population in the southern GBR was associated with a symbiont taxon of the C50b subclade. A few colonies at Lady Musgrave Island were associated with C3k. Corals in western NC were predominantly associated with a taxon from the C3k/C3bo subclade. The exception was some colonies on most southern reefs, which were associated with a distinct symbiont taxon from the C50b subclade. Based on ITS2 profiles, *k*-mer profile clustering, and geographic separation, this symbiont taxon is genetically differentiated from the C50b taxa found in the southern GBR (Figures S5 and S6). Coral hosts in the CB atolls were also associated with a C3k/C3bo taxon that was indistinguishable from NC C3k/C3bo based on *k*-mer profiles, despite being separated by >400 km (Figure S5C).

Drivers of host and symbiont genetic structure

The redundancy analysis (RDA) indicated that environmental variables significantly predicted coral host genetic structure (ANOVA; $p < 0.01$), explaining 64% of the total variance. Maximum monthly mean (MMM) sea temperature, the frequency of mild marine heatwaves (DHW > 4), and distance to coast were the strongest reef-level environmental predictors of host population structure (cumulative adjusted $R^2 = 0.60$; Table 2). A global RDA, including geographic predictors (distance-based Moran's Eigenvector maps; dbMEMs) in addition to significant environmental variables, explained 70% of the total variance in host genetic structure. Due to the spatial sampling design, several partial RDAs indicated that environmental and geographic effects were largely confounded (86% of the explained variance).

Environmental predictors also significantly influenced the community composition of *Cladocopium* symbionts (ANOVA; $p < 0.01$), explaining 37% of the total variance (Table 2). The MMM, frequency of mild marine heatwaves (DHW > 4), and annual range in sea surface temperature (AR) were retained as significant predictors in the model ($p = 0.001$). The AR separated C3 populations, found in more thermally variable environments at inshore and high-latitude reefs, from C50 populations found in offshore and low-latitude reefs (Figure 4B). Within the C50 subclade, distinct C50b and C50c populations were separated primarily by the MMM, reflecting both temperature variation across the latitudinal gradient and cross-shore gradients. Within the C3 subclade, the C3k populations were positively associated with the MMM, while C3k/C3bo populations were found in reefs where MMM was lower on average, but where mild marine heatwaves have been more frequent. Several partial redundancy analyses (pRDAs) indicated that environment was the strongest driver of symbiont community composition (6.3% of total explained variance). Geography (1.2%) and host population structure (1%) were less influential, although the effect of these three components was also largely confounded (80% of the explained variance; Table 2).

DISCUSSION

Our results revealed four genetically distinct *A.* cf. *spathulata* populations in the studied western Pacific region, which have

Table 2. Influence of geography and environmental conditions on coral host genetic structure and associated Symbiodiniaceae communities

Partial RDA models	Inertia	R^2 (total variance explained)	$p(>F)$	Proportion of constrained variance explained
Host model				
Host PC ~ Env + geography	21.38	0.701	0.001***	1
Host PC ~ geography|Env	1.898	0.06	0.001***	0.089
Host PC ~ Env|geography	0.987	0.03	0.001***	0.046
Confounded Env/geography	–	0.611	–	0.865
Total unexplained	9.08	0.29	–	–
Total inertia	30.46	1	–	–
Symbiont model				
k-mer ~ Env + geography + Host_structure|(Nreads)	0.174	0.40	0.01**	1
k-mer ~ Env|(Nreads + Host_structure + geography)	0.027	0.063	0.01**	0.15
k-mer ~ geography|(Nreads + Env + host structure)	0.005	0.012	0.01**	0.03
k-mer ~ Host_structure|(Nreads + Env + geography)	0.004	0.01	0.01**	0.02
Confounded Env/geography/host structure	–	0.315	–	0.8
Total unexplained	0.167	0.6	–	–
Total inertia	0.435	1	–	–

The host model evaluates the influence of geography and environmental conditions on host genetic structure of *Acropora* cf. *spathulata*. The symbiont model evaluates the influence of geography, environmental conditions, and host genetic structure on associated Symbiodiniaceae communities. The relative influence of each category of predictors was decomposed using partial redundancy analysis (pRDA). Geography was modeled using dbMEMs. Environmental conditions were represented by predictors encompassing temperature, irradiance, and turbidity. $^{**}p \leq 0.01$, $^{***}p \leq 0.001$. See also Figure S1 and Table S5.

diverged due to geographic isolation but maintain gene flow through major oceanographic currents. These populations show little genetic structure over distances greater than 500 km, reflecting a generational dispersal distance estimated at ~100 km. In contrast, coral hosts are associated with distinct algal symbionts of five Symbiodiniaceae taxa across shorter latitudinal and cross-shelf gradients. This study presents one of the most extensive datasets for analyzing spatial genetic variation in both corals and their algal symbionts based on whole-genome sequences, combining broad geographic coverage and dense local sampling. These results suggest that large local populations and dispersal support resilience of a broadcast-spawning coral, whereas habitat-specific symbionts and long-distance gene flow could enhance its adaptive potential in changing environments.

Regional spatial genetic variation differs among holobiont partners

The spatial scale of genetic variation differed markedly between *A.* cf. *spathulata* and its associated *Symbiodiniaceae*. This coral species comprised four genetically differentiated populations distributed in distinct regions separated by ~600–2,200 km. However, each population was largely genetically homogeneous based on PCA, ADMIXTURE, and IbD analyses, despite spanning up to >300 km for NC and CB and up to >500 km for the central/northern GBR. Conversely, Symbiodiniaceae community genetic variation occurred over spatial scales as small as 30 km, and colonies from the same reef sometimes hosted distinct symbiont taxa. These patterns reflect the predominant effect of distinct evolutionary forces acting on holobiont partners.

Patterns of *A.* cf. *spathulata* genetic variation suggest that extensive gene flow promotes genetic homogenization of populations, counteracting the effects of drift and local adaptation.[73] This was supported by our estimated σ exceeding 100 km. Across the distant western Pacific populations, reduced gene flow and increasing environmental contrasts (e.g., Δ~3°C in MMM; Figure S1B) drive greater genetic differentiation (D_{xy} = 0.0102–0.0107). However, the relative importance of genetic drift and local adaptation in this differentiation could not be disentangled due to spatial confounding between environmental and geographic predictors (Table 2). Future studies integrating morphological and genomic data (e.g., Rassmussen et al.[6] and Bridge et al.[74]) across a broader geographic range, including populations from the *A. spathulata* holotype locality in the Solomon Islands, will be necessary to determine whether the lineage described here represents a synonymized species or populations of the same species.

Patterns of Symbiodiniaceae genetic variation suggest that environmental filtering is the predominant driver of *A.* cf. *spathulata* algal symbioses. Variation in symbiont communities was likely not strongly influenced by dispersal, as it did not follow an IbD pattern. For instance, colonies from Martin and No Name reefs (30 km apart) hosted different taxa, while those from No Name and Chicken reefs hosted the same taxa (500 km apart; Figure 4). In addition, the environment had a larger

effect on symbioses than host genetic differentiation (although largely confounded; pRDA; Table 2), as expected from species that acquire symbionts from their environment after settlement.[46,54] Variation in symbioses was particularly pronounced across shelf and latitudinal gradients, similar to other *Acropora* species on the GBR.[50,51,53] Notably, *A.* cf. *spathulata* and *A. tersa*[6] (a recently named species of the *A. hyacinthus* species complex) hosted strikingly similar Symbiodiniaceae communities, with identical ITS2 types found across comparable environmental gradients.[52] RDAs suggest that temperature was the primary driver, although other important factors, such as light and turbidity,[75] were likely excluded due to multicollinearity. It also remains unclear whether *A.* cf. *spathulata* associates with specific Symbiodiniaceae because these taxa are locally abundant and/or they form the best performing symbioses.[42]

The spatial distribution of Symbiodiniaceae suggests that some taxa may be environmental specialists while others may be environmental generalists. Similar to Epstein et al.,[76] we found *A.* cf. *spathulata* associated with a C3k taxon at cooler offshore central/northern GBR reefs, and we also revealed a distinct C50c taxon predominant at warmer turbid inshore central/northern reefs. Conversely, C3k/C3bo appears to have a wide distribution as it was indistinguishable based on genome-sequence composition between NC and CB. Taxa from the C50b subclade, found across a 13° longitudinal gradient, might also be widespread in this region but best performing at high latitudes. Our findings reinforce the idea that niche partitioning can promote ecological diversification of closely related algal symbionts,[77,78] as the C50c and C50b populations were found in warmer and cooler environments, respectively. Importantly, additional genetic diversity within major Symbiodiniaceae taxa may result from local adaptation of symbiont populations and/or genotypes,[43] potentially explaining the diversity of ITS2 profiles observed within taxa (Figure S6A). Such fine-scale genetic variation was not detected by the alignment-free approach and may require tailored methods, including microsatellite analyses[79] or the retrieval of chloroplast SNPs.[48]

Broadcast spawners maintain long-distance asymmetrical gene flow across the western Pacific

Demographic models detected substantial historical gene flow between western Pacific populations separated by thousands of kilometers, which likely started to diverge between 0.275 and 0.651 mya. Although this potential connectivity had been suggested by biophysical models of coral dispersal,[80] it remained to be empirically tested, as these approaches can be biased at coarse spatial resolutions.[81] Although some uncertainty remained in the absolute values of gene flow, the primary directions of migration rates were consistent across bootstrap replicates for all population pairs, and these models had stronger support than divergence without gene flow.

On the GBR, gene flow was primarily southward, consistent with the predominant East Australian Current (EAC) direction and other studies on coral broadcast spawners.[18,30,55] We also observed admixture between the central/northern and southern GBR populations, indicating recent southward migration between these regions (Figure 1). Conversely, gene flow was largely symmetrical between the GBR and Coral Sea atolls, reflecting the region's complex oceanography, which includes westward currents such as the North Caledonia Jet (NCJ) and the South Caledonia Jet (SCJ),[61] as well as the eastward Subtropical Counter Current (STCC).[82] Demographic models inferred dominant eastward gene flow from the GBR to NC, and from CB to NC, which is unexpected given the prevailing westward NCJ and SCJ in the region.[61] These patterns of realized connectivity may have been influenced by surface circulation associated with the STCC, while the strong NCJ and SCJ reach their maximum intensity in deeper layers.[82] Observations of plastic debris and Lagrangian dispersal modeling notably suggest that mesoscale currents can generate eastward drift in the region despite the dominance of westward zonal jets.[83] Because gene flow inferred from demographic models reflects an average across thousands of generations, these estimates could also have been influenced by temporal changes in ocean circulation. Together, these results provide novel insights into complex realized connectivity across this region and highlight the value of such analyses for informing management in contexts of variable ocean circulation. Beyond uncertainties in the current directionality of gene flow, the models strongly support low but persistent migration between these western Pacific populations. As such, they should be treated as distinct management units[84] within a broader regional network that also recognizes the importance of their connectivity for evolutionary adaptive potential.

Large breeding population and high dispersal may support demographic resilience

The effective population size of *A.* cf. *spathulata* at the neighborhood size was relatively high (N_e = 2,950) despite drastic coral mortality over past decades.[1,85] This estimate is particularly important for conservation, as emphasized in the recent Kunming-Montreal Global Biodiversity Framework.[22] Although there is no exact rule for how large N_e should be, our estimate suggests that local breeding populations are sufficiently large to prevent dramatic loss of genetic diversity due to genetic drift.[22] In contrast, brooding species with limited dispersal and local recruitment tend to have lower N_e and higher local extinction risk.[18,19,24]

High N_e likely reflects substantial census sizes of this common species densely distributed on reef flats and slopes, combined with a large generation dispersal estimated at ~100 km per generation. This estimate contains some level of uncertainty because IbD theory assumes symmetrical dispersal across a continuous habitat of constant population density, which does not match the typical patchiness of coral reefs. Yet this value is consistent with a pelagic larval duration estimated from lipid reserves at ~100 days, which would allow larvae to be carried across large distances.[86] Estimates from previous studies using similar methods vary from a few meters in brooding species[19,20,24] to 1–52 km in broadcast-spawning species.[18,21] Our estimate also falls at the upper end of broadcast-spawners connectivity predicted by biophysical models (63% of settlement within 100 km)[80] and is comparable to coral trout dispersal on the GBR.[87] These findings suggest that *A.* cf. *spathulata* exhibits one of the highest coral dispersal distances recorded to date. Importantly, we only estimated a global isotropic σ because IbD was not significant within populations, but this estimate could vary among regions. Even if σ is similar across regions, the demographic consequences could differ because the GBR is a

fragmented mosaic of numerous discrete reefs, while NC and CB contain longer continuous barrier reefs.[88] Individual reefs are expected to be demographically isolated when separated by more than 2σ,[89] and thus connectivity could differ between these reef systems of contrasting geomorphology.

Large N_e and high dispersal may explain the impressive recovery of *Acropora* communities on many GBR reefs after the 2016–2017 bleaching-related mortality events[90] and will be critical for demographic recovery under increasingly frequent disturbances.[14] For example, marine heatwaves and freshwater floods caused 90%–100% mortality of *A.* cf. *spathulata* colonies at several inshore northern GBR sites sampled in this study in 2024, whereas colonies at offshore reefs were relatively unaffected. Larval dispersal from these populations could thus in theory supply larvae to degraded reefs. However, a finer assessment of realized dispersal is needed to evaluate the inbound and outbound connectivity of individual reefs, as it depends on mesoscale currents and habitat availability. Finally, given the ongoing impacts to these populations from global warming, monitoring possible changes in N_e will be important for tracking changes in their vulnerability.[91]

Habitat-specific symbioses and long-range dispersal affect the evolutionary adaptive potential of *A.* cf. *spathulata*

A. cf. *spathulata* formed distinct symbioses with Symbiodiniaceae across distinct thermal conditions, which raises the question of whether a shift to more heat-tolerant symbioses could promote the adaptation of *A.* cf. *spathulata* to rapid climate warming. *Acropora* corals symbioses with heat-tolerant symbionts—notably from the *Durusdinium* genus—have been observed to increase in prevalence during marine heatwaves, but this response appears to be species specific and has not yet been reported for *A.* cf. *spathulata*.[92] The absence of *Durusdinium* in colonies sampled outside major marine heatwaves in Epstein et al.[76] and in our study suggests this association is uncommon in *A.* cf. *spathulata* under normal conditions. However, we observed variable symbioses among colonies at mid-shelf reefs on the GBR, suggesting that both the C50c and C3k taxa are found in these environments. Under future climate warming, symbioses with C50c, typically found in warmer inshore environments, may become more prevalent on mid-shelf reefs, especially given that fast-growing *Acropora* corals can rapidly shift to better-adapted symbionts within 1–2 years.[93] Whether this ability varies across regions remains an open question, especially given that the same C3k/C3bo taxon was found in colonies both from NC and CB reefs despite drastically different environments. The absence of other associations may indicate lower potential for adaptation through shifts in symbioses or, on the contrary, indicate greater physiological plasticity and resilience to changing conditions of this symbiont taxon. Further sampling around bleaching events is thus needed to assess whether this species can shift symbioses quickly enough to reduce coral mortality over future marine heatwaves.

Another factor that may underlie the evolutionary adaptation of *A.* cf. *spathulata* is the long-distance gene flow between western Pacific populations, as it could increase genetic variation or introduce heat-tolerant alleles from warmer to cooler regions.[67] On the GBR, dominant southward gene flow may allow this process, as observed in other coral taxa,[18,30,55] particularly given that admixture suggests recent southward migration. Among other populations, the effect of gene flow on adaptive genetic variation may be harder to predict due to more complex patterns. For example, the southern GBR showed substantial northeastward gene flow toward CB populations typically found in warmer environments. Nevertheless, occasional long-distance gene flow will benefit populations' adaptive potential by introducing novel genetic variation without swamping adaptive local variants.[94] We only inferred broadscale patterns of gene flow among the four regions. Sampling a continuum of reefs in these regions and modeling gene flow at a finer resolution among reef groups (e.g., Meziere et al.[18] and Matz et al.[30]), along with construction of high-resolution biophysical models (e.g., Mason et al.[95]), would help build finer networks of reef connectivity.[96]

Within regions, high levels of gene flow will constrain evolution by preventing strong local adaptation, for instance along cross-shore gradients. However, it will also facilitate the spread of standing genetic variation, as evidenced by limited differences in genetic diversity between reefs and regions. This gene flow will reduce the risk of inbreeding depression and enable the rapid spread of novel genetic variants across the population range.[73] Future work investigating the distribution of adaptive genetic variation in this species will help clarify this ambivalent effect.

Conclusions

The genetic structure of the western Pacific coral *A.* cf. *spathulata* reflects opposing forces of geographic isolation and long-distance dispersal driven by major regional ocean currents. In parallel, variation in associated *Cladocopium* taxa along latitudinal and cross-shore environmental gradients suggests environmental filtering of symbioses. Our results enable the definition of management units across the western Pacific and emphasize the importance of considering coral reefs' connectivity at the regional scale beyond national borders—as maintaining gene flow between distant populations could underlie their evolutionary adaptation.[94] The distinct spatial scales at which evolutionary processes affect coral hosts and their symbionts are also essential to consider for many proposed intervention approaches, such as assisted gene flow, selective breeding, or symbiont manipulations.[97] Our findings indicate substantial effective population size and exceptional dispersal in *A.* cf. *spathulata* that may support demographic rescue following disturbances, provided some locations remain unaffected. However, this study only offers a snapshot of the demographic status of *A.* cf. *spathulata* populations. In light of recent severe coral mortality events,[98] future reassessment of their vulnerability will be essential for effective conservation.

RESOURCE AVAILABILITY

Lead contact

Requests for further information and resources should be directed to and will be fulfilled by the lead contact, Hugo Denis (denis.hugo08@gmail.com).

Materials availability

This study did not generate new, unique reagents.

Data and code availability

- Raw sequencing data for whole-genome sequencing (WGS) are available through NCBI (BioProject PRJNA1390968 and BioProject PRJNA1357023), and associated sample metadata and pictures can

be accessed on GEOME (https://n2t.net/ark:/21547/R2658 and https://n2t.net/ark:/21547/R2650). ITS2 amplicon sequencing data are available through Symportal (20250122T050733_denishu1).
- All original code and scripts used for WGS data processing and analyses are available on GitHub (https://github.com/hde08/Aspat_WesternPacific_Popgen) and are archived on Zenodo (https://doi.org/10.5281/zenodo.18263493).
- Any additional information required to reanalyze the data reported in this paper is available from the lead contact upon request.

ACKNOWLEDGMENTS

Work undertaken in Australia was supported by the Reef Restoration and Adaptation Program, funded through a partnership between the Australian Government's Reef Trust and the Great Barrier Reef Foundation. Work in New Caledonia was supported by CNRS and IRD funding and was part of the WINREEF (Reef Resilient Initiative/ Neo Caledonia Biodiversity Agency funding) and ReCoVer (Pacific Funds) projects. Sampling at CB was conducted with the support of the French Navy aboard the vessel *D'Entrecasteaux*. H.D. was supported by a PhD scholarship from ED129 at Sorbonne University. H.I. and I.B were supported by the University of Queensland Research Training Program scholarship. We thank the Traditional Owners of the Great Barrier Reef and New Caledonia reefs for their free, prior, and informed consent to undertake coral sampling in their Sea Country. We thank the Government of New Caledonia for granting permission to conduct coral sampling within the Natural Park of the Coral Sea, as well as the South Province and North Province. We thank Samantha Goyen, Riverside Marine Cruise crew members, and numerous AIMS staff and volunteers for their support during sampling on the GBR. We thank the French National Navy, Mahé Dumas, Bertrand Bourgeois, William Roman, Jordi Giraud, and Martin Nguyen for their help during sampling in the Chesterfield-Bellona atolls and New Caledonia Grande Terre. We thank Samantha Howitt for assisting with the DNA extractions at the University of Queensland and Clarisse Majorel for assisting with the DNA extractions in New Caledonia. We thank Molly Przeworski for providing an upgraded reference genome assembly. We thank Jérôme Lefèvre and Christophe Charbuillet for their support with HPC systems. This research was undertaken with the assistance of resources from the National Computational Infrastructure (NCI Australia), an NCRIS-enabled capability supported by the Australian Government, through Project d85 awarded to C.X.C. Finally, we are grateful to Ryan Gutenkunst for his advice on demographic modeling analyses.

AUTHOR CONTRIBUTIONS

V.B.-L., E.J.H., L.K.B., C.R., and H.D. initiated the project and planned the sampling campaign. Fieldwork was done by H.D., L.K.B., V.J.L.M., and E.J.H. on the GBR and H.D., V.B.-L., M.B., and G.L. in New Caledonia. DNA extractions were performed by I.B. and K.E.P. for GBR samples and by H.D. for New Caledonia samples. Whole-genome sequence data were curated and analyzed by H.D. following a pipeline designed by I.P. Host population structure and phylogenetic analyses were performed by H.D., supported by I.P., K.E.P., C.R., E.J.H., G.L., and V.B.-L. Demographic modeling analyses were performed by H.D., supported by K.E.P. IbD analyses were performed by K.E.P. Analyses of symbiont communities were performed by H.D., supported by H.I. and C.X.C. H.D. wrote the first draft version of the manuscript, which was critically revised by all co-authors. All authors read and approved the final manuscript.

DECLARATION OF INTERESTS

The authors declare no competing interests.

STAR★METHODS

Detailed methods are provided in the online version of this paper and include the following:

- KEY RESOURCES TABLE
- EXPERIMENTAL MODEL AND STUDY PARTICIPANT DETAILS
  - Study sites and sample collection
- METHOD DETAILS
  - DNA extraction and sequencing
  - Genomic data pre-variant processing and filtering
  - Choice of reference genome
  - SNP calling, clone identification and filtering
  - Testing for batch effects
  - Host population genomic using genotype likelihoods
  - Validation of differentiation from *A. millepora*
  - Clones and related individuals' identification
  - Host population genomics analyses
  - Demographic modeling
  - Symbiodiniaceae community analyses
  - Host and symbiont co-clustering analysis
  - Environmental data acquisition
- QUANTIFICATION AND STATISTICAL ANALYSIS
  - Population statistics
  - Isolation by distance analysis and estimating N_e
  - Distance based redundancy analysis

SUPPLEMENTAL INFORMATION

Supplemental information can be found online at https://doi.org/10.1016/j.cub.2026.04.057.

Received: October 14, 2025
Revised: February 2, 2026
Accepted: April 24, 2026
Published: May 20, 2026

REFERENCES

1. Souter, D., Planes, S., Wicquart, J., Logan, M., Obura, D., and Staub, F. (2021). Status of coral reefs of the world: 2020 (Global Coral Reef Monitoring Network [GCRMN] and International Coral Reef Initiative [ICRI]). https://gcrmn.net/wp-content/uploads/2023/01/Status-of-Coral-Reefs-of-the-World-2020-Full-Report.pdf.
2. Edmunds, P.J., and Riegl, B. (2020). Urgent need for coral demography in a world where corals are disappearing. Mar. Ecol. Prog. Ser. *635*, 233–242. https://doi.org/10.3354/meps13205.
3. van Oppen, M.J.H., and Gates, R.D. (2006). Conservation genetics and the resilience of reef-building corals. Mol. Ecol. *15*, 3863–3883. https://doi.org/10.1111/j.1365-294X.2006.03026.x.
4. Riginos, C., Popovic, I., Meziere, Z., Garcia, V., Byrne, I., Howitt, S.M., Ishida, H., Bairos-Novak, K., Humanes, A., Scharfenstein, H., et al. (2024). Cryptic species and hybridisation in corals: challenges and opportunities for conservation and restoration. Peer Community J. *4*, e106. https://doi.org/10.24072/pcjournal.492.
5. Grupstra, C.G.B., Gómez-Corrales, M., Fifer, J.E., Aichelman, H.E., Meyer-Kaiser, K.S., Prada, C., and Davies, S.W. (2024). Integrating cryptic diversity into coral evolution, symbiosis and conservation. Nat. Ecol. Evol. *8*, 622–636. https://doi.org/10.1038/s41559-023-02319-y.
6. Rassmussen, S.H., Cowman, P.F., Baird, A.H., Crosbie, A.J., Quattrini, A.M., Bonito, V., Sinniger, F., Harii, S., Cabaitan, P.C., Fadli, N., et al. (2025). The tables have turned: taxonomy, systematics and biogeography of the *Acropora hyacinthus* (Scleractinia: Acroporidae) complex. Invertebr. Syst. *39*, IS24049. https://doi.org/10.1071/IS24049.
7. Ramírez-Portilla, C., Baird, A.H., Cowman, P.F., Quattrini, A.M., Harii, S., Sinniger, F., and Flot, J.-F. (2022). Solving the coral species delimitation conundrum. Syst. Biol. *71*, 461–475. https://doi.org/10.1093/sysbio/syab077.
8. Gleason, D.F., and Hofmann, D.K. (2011). Coral larvae: from gametes to recruits. J. Exp. Mar. Biol. Ecol. *408*, 42–57. https://doi.org/10.1016/j.jembe.2011.07.025.

9. Bourne, D.G., Morrow, K.M., and Webster, N.S. (2016). Insights into the coral microbiome: underpinning the health and resilience of reef ecosystems. Annu. Rev. Microbiol. *70*, 317–340. https://doi.org/10.1146/annurev-micro-102215-095440.

10. Bongaerts, P., Cooke, I.R., Ying, H., Wels, D., den Haan, S., Hernandez-Agreda, A., Brunner, C.A., Dove, S., Englebert, N., Eyal, G., et al. (2021). Morphological stasis masks ecologically divergent coral species on tropical reefs. Curr. Biol. *31*, 2286–2298.e8. https://doi.org/10.1016/j.cub.2021.03.028.

11. Meziere, Z., Popovic, I., Prata, K., Ryan, I., Pandolfi, J., and Riginos, C. (2024). Exploring coral speciation: Multiple sympatric *Stylophora pistillata* taxa along a divergence continuum on the Great Barrier Reef. Evol. Appl. *17*, e13644. https://doi.org/10.1111/eva.13644.

12. Arrigoni, R., Berumen, M.L., Mariappan, K.G., Beck, P.S.A., Hulver, A.M., Montano, S., Pichon, M., Strona, G., Terraneo, T.I., and Benzoni, F. (2020). Towards a rigorous species delimitation framework for scleractinian corals based on RAD sequencing: the case study of *Leptastrea* from the Indo-Pacific. Coral Reefs *39*, 1001–1025. https://doi.org/10.1007/s00338-020-01924-8.

13. Fuentes-Pardo, A.P., and Ruzzante, D.E. (2017). Whole-genome sequencing approaches for conservation biology: Advantages, limitations and practical recommendations. Mol. Ecol. *26*, 5369–5406. https://doi.org/10.1111/mec.14264.

14. Hock, K., Wolff, N.H., Ortiz, J.C., Condie, S.A., Anthony, K.R.N., Blackwell, P.G., and Mumby, P.J. (2017). Connectivity and systemic resilience of the Great Barrier Reef. PLoS Biol. *15*, e2003355. https://doi.org/10.1371/journal.pbio.2003355.

15. Holbrook, S.J., Adam, T.C., Edmunds, P.J., Schmitt, R.J., Carpenter, R.C., Brooks, A.J., Lenihan, H.S., and Briggs, C.J. (2018). Recruitment drives spatial variation in recovery rates of resilient coral reefs. Sci. Rep. *8*, 7338. https://doi.org/10.1038/s41598-018-25414-8.

16. Wright, S. (1946). Isolation by distance under diverse systems of mating. Genetics *31*, 39–59. https://doi.org/10.1093/genetics/31.1.39.

17. Rousset, F. (1997). Genetic differentiation and estimation of gene flow from F-statistics under isolation by distance. Genetics *145*, 1219–1228. https://doi.org/10.1093/genetics/145.4.1219.

18. Meziere, Z., Prata, K., Lechene, M., Ferrari, R., Popovic, I., and Riginos, C. (2025). Connectivity differs by orders of magnitude among co-distributed corals, affecting spatial scales of eco-evolutionary processes. Sci. Adv. *11*, eadt2066. https://doi.org/10.1126/sciadv.adt2066.

19. Prata, K.E., Bongaerts, P., Dwyer, J.M., Ishida, H., Howitt, S.M., Hereward, J.P., Crandall, E.D., and Riginos, C. (2024). Some reef-building corals only disperse metres per generation. Proc. Biol. Sci *291*, 20231988.

20. Gorospe, K.D., and Karl, S.A. (2013). Genetic relatedness does not retain spatial pattern across multiple spatial scales: Dispersal and colonization in the coral, *Pocillopora damicornis*. Mol. Ecol. *22*, 3721–3736. https://doi.org/10.1111/mec.12335.

21. Japaud, A., Bouchon, C., Magalon, H., and Fauvelot, C. (2019). Geographic distances and ocean currents influence Caribbean *Acropora palmata* population connectivity in the Lesser Antilles. Conserv. Genet. *20*, 447–466. https://doi.org/10.1007/s10592-019-01145-9.

22. Waples, R. (2024). The Idiot's Guide to Effective Population Size (Authorea Inc), pp. 1–51.

23. Fisher, R.A. (1930). The Genetical Theory of Natural Selection (Clarendon Press). https://doi.org/10.5962/bhl.title.27468.

24. Hernández-Agreda, A., Huckeba, J., Prata, K.E., Vermeij, M.J.A., and Bongaerts, P. (2024). Hybridization and inbreeding affect the survival of a critically endangered coral. Curr. Biol. *34*, 5120–5129.e4. https://doi.org/10.1016/j.cub.2024.09.035.

25. Gaines, S.D., White, C., Carr, M.H., and Palumbi, S.R. (2010). Designing marine reserve networks for both conservation and fisheries management. Proc. Natl. Acad. Sci. USA *107*, 18286–18293. https://doi.org/10.1073/pnas.0906473107.

26. Clobert, J. (2012). Dispersal Ecology and Evolution (Oxford University Press).

27. Lawson, D.J., Van Dorp, L., and Falush, D. (2018). A tutorial on how not to over-interpret STRUCTURE and ADMIXTURE bar plots. Nat. Commun. *9*, 3258. https://doi.org/10.1038/s41467-018-05257-7.

28. Whitlock, M.C., and McCauley, D.E. (1999). Indirect measures of gene flow and migration: FST≠1/(4Nm+ 1). Heredity *82*, 117–125. https://doi.org/10.1038/sj.hdy.6884960.

29. Gutenkunst, R.N., Hernandez, R.D., Williamson, S.H., and Bustamante, C.D. (2009). Inferring the joint demographic history of multiple populations from multidimensional SNP frequency data. PLoS Genet. *5*, e1000695. https://doi.org/10.1371/journal.pgen.1000695.

30. Matz, M.V., Treml, E.A., Aglyamova, G.V., and Bay, L.K. (2018). Potential and limits for rapid genetic adaptation to warming in a Great Barrier Reef coral. PLoS Genet. *14*, e1007220. https://doi.org/10.1371/journal.pgen.1007220.

31. Davies, S.W., Treml, E.A., Kenkel, C.D., and Matz, M.V. (2015). Exploring the role of Micronesian islands in the maintenance of coral genetic diversity in the Pacific Ocean. Mol. Ecol. *24*, 70–82. https://doi.org/10.1111/mec.13005.

32. Zhang, J., Richards, Z.T., Adam, A.A.S., Chan, C.X., Shinzato, C., Gilmour, J., Thomas, L., Strugnell, J.M., Miller, D.J., and Cooke, I. (2022). Evolutionary responses of a reef-building coral to climate change at the end of the last glacial maximum. Mol. Biol. Evol. *39*, msac201. https://doi.org/10.1093/molbev/msac201.

33. Tsuchiya, K., Zayasu, Y., Nakajima, Y., Arakaki, N., Suzuki, G., Satoh, N., and Shinzato, C. (2022). Genomic analysis of a reef-building coral, *Acropora digitifera*, reveals complex population structure and a migration network in the Nansei Islands, Japan. Mol. Ecol. *31*, 5270–5284. https://doi.org/10.1111/mec.16665.

34. Colton, M.A., McManus, L.C., Schindler, D.E., Mumby, P.J., Palumbi, S.R., Webster, M.M., Essington, T.E., Fox, H.E., Forrest, D.L., Schill, S.R., et al. (2022). Coral conservation in a warming world must harness evolutionary adaptation. Nat. Ecol. Evol. *6*, 1405–1407. https://doi.org/10.1038/s41559-022-01854-4.

35. LaJeunesse, T.C., Parkinson, J.E., Gabrielson, P.W., Jeong, H.J., Reimer, J.D., Voolstra, C.R., and Santos, S.R. (2018). Systematic revision of Symbiodiniaceae highlights the antiquity and diversity of coral endosymbionts. Curr. Biol. *28*, 2570–2580.e6. https://doi.org/10.1016/j.cub.2018.07.008.

36. Nitschke, M.R., Rosset, S.L., Oakley, C.A., Gardner, S.G., Camp, E.F., Suggett, D.J., and Davy, S.K. (2022). The diversity and ecology of Symbiodiniaceae: A traits-based review. Adv. Mar. Biol. *92*, 55–127. https://doi.org/10.1016/bs.amb.2022.07.001.

37. Levin, R.A., Beltran, V.H., Hill, R., Kjelleberg, S., McDougald, D., Steinberg, P.D., and van Oppen, M.J.H. (2016). Sex, scavengers, and chaperones: transcriptome secrets of divergent *Symbiodinium* thermal tolerances. Mol. Biol. Evol. *33*, 2201–2215. https://doi.org/10.1093/molbev/msw119.

38. McRae, C.J., Keshavmurthy, S., Chen, H.-K., Ye, Z.-M., Meng, P.-J., Rosset, S.L., Huang, W.-B., Chen, C.A., Fan, T.-Y., and Côté, I.M. (2023). Baseline dynamics of Symbiodiniaceae genera and photochemical efficiency in corals from reefs with different thermal histories. PeerJ *11*, e15421. https://doi.org/10.7717/peerj.15421.

39. LaJeunesse, T.C., Smith, R.T., Finney, J., and Oxenford, H. (2009). Outbreak and persistence of opportunistic symbiotic dinoflagellates during the 2005 Caribbean mass coral 'bleaching' event. Proc. R. Soc. B. *276*, 4139–4148. https://doi.org/10.1098/rspb.2009.1405.

40. Reich, H.G., Kitchen, S.A., Stankiewicz, K.H., Devlin-Durante, M., Fogarty, N.D., and Baums, I.B. (2021). Genomic variation of an endosymbiotic dinoflagellate (*Symbiodinium* 'fitti') among closely related coral hosts. Mol. Ecol. *30*, 3500–3514. https://doi.org/10.1111/mec.15952.

41. Quigley, K.M., Willis, B.L., and Kenkel, C.D. (2019). Transgenerational inheritance of shuffled symbiont communities in the coral *Montipora digitata*. Sci. Rep. *9*, 1–11. https://doi.org/10.1038/s41598-019-50045-y.

42. Bhattacharya, D., Stephens, T.G., Chille, E.E., Benites, L.F., and Chan, C.X. (2024). Facultative lifestyle drives diversity of coral algal symbionts. Trends Ecol. Evol. *39*, 239–247. https://doi.org/10.1016/j.tree.2023.10.005.

43. Howells, E.J., Beltran, V.H., Larsen, N.W., Bay, L.K., Willis, B.L., and van Oppen, M.J.H. (2012). Coral thermal tolerance shaped by local adaptation of photosymbionts. Nat. Clim. Change *2*, 116–120. https://doi.org/10.1038/nclimate1330.

44. Hume, B.C.C., Smith, E.G., Ziegler, M., Warrington, H.J.M., Burt, J.A., LaJeunesse, T.C., Wiedenmann, J., and Voolstra, C.R. (2019). SymPortal: A novel analytical framework and platform for coral algal symbiont next-generation sequencing ITS2 profiling. Mol. Ecol. Resour. *19*, 1063–1080. https://doi.org/10.1111/1755-0998.13004.

45. Moore, R.B., Ferguson, K.M., Loh, W.K., Hoegh-Guldberg, O., and Carter, D.A. (2003). Highly organized structure in the non-coding region of the psbA minicircle from clade C *Symbiodinium*. Int. J. Syst. Evol. Microbiol. *53*, 1725–1734. https://doi.org/10.1099/ijs.0.02594-0.

46. Davies, S.W., Moreland, K.N., Wham, D.C., Kanke, M.R., and Matz, M.V. (2020). *Cladocopium* community divergence in two *Acropora* coral hosts across multiple spatial scales. Mol. Ecol. *29*, 4559–4572. https://doi.org/10.1111/mec.15668.

47. Lewis, A.M., Butler, C.C., Turnham, K.E., Wham, D.F., Hoadley, K.D., Smith, R.T., Kemp, D.W., Warner, M.E., and LaJeunesse, T.C. (2024). The diversity, distribution, and temporal stability of coral 'zooxanthellae' on a pacific reef: from the scale of individual colonies to across the host community. Coral Reefs *43*, 841–856. https://doi.org/10.1007/s00338-024-02503-x.

48. Armstrong, K.C., Lippert, M., Hanson, E., Nestor, V., Cornwell, B., Walker, N.S., Golbuu, Y., and Palumbi, S.R. (2024). Fine-scale geographic variation of *Cladocopium* in *Acropora hyacinthus* across the Palauan archipelago. Ecol. Evol. *14*, e70650. https://doi.org/10.1002/ece3.70650.

49. Ishida, H., Riginos, C., and Chan, C.X. (2024). Contaminant or goldmine? In silico assessment of Symbiodiniaceae community using coral hologenomes. Front. Protistol. *2*, 1376877. https://doi.org/10.3389/frpro.2024.1376877.

50. Cooke, I., Ying, H., Forêt, S., Bongaerts, P., Strugnell, J.M., Simakov, O., Zhang, J., Field, M.A., Rodriguez-Lanetty, M., Bell, S.C., et al. (2020). Genomic signatures in the coral holobiont reveal host adaptations driven by Holocene climate change and reef specific symbionts. Sci. Adv. *6*, eabc6318. https://doi.org/10.1126/sciadv.abc6318.

51. Matias, A.M.A., Popovic, I., Thia, J.A., Cooke, I.R., Torda, G., Lukoschek, V., Bay, L.K., Kim, S.W., and Riginos, C. (2022). Cryptic diversity and spatial genetic variation in the coral *Acropora tenuis* and its endosymbionts across the Great Barrier Reef. Evol. Appl. *16*, 293–310. https://doi.org/10.1111/eva.13435.

52. Naugle, M.S., Denis, H., Mocellin, V.J.L., Laffy, P.W., Popovic, I., Bay, L.K., and Howells, E.J. (2024). Heat tolerance varies considerably within a reef-building coral species on the Great Barrier Reef. Commun. Earth Environ. *5*, 525. https://doi.org/10.1038/s43247-024-01649-4.

53. LaJeunesse, T., Bhagooli, R., Hidaka, M., DeVantier, L., Done, T., Schmidt, G., Fitt, W., and Hoegh-Guldberg, O. (2004). Closely related *Symbiodinium* spp. differ in relative dominance in coral reef host communities across environmental, latitudinal and biogeographic gradients. Mar. Ecol. Prog. Ser. *284*, 147–161. https://doi.org/10.3354/meps284147.

54. van Oppen, M.J.H., Palstra, F.P., Piquet, A.M.-T., and Miller, D.J. (2001). Patterns of coral–dinoflagellate associations in *Acropora*: significance of local availability and physiology of *Symbiodinium* strains and host–symbiont selectivity. Proc. R. Soc. Lond. B *268*, 1759–1767. https://doi.org/10.1098/rspb.2001.1733.

55. Riginos, C., Hock, K., Matias, A.M., Mumby, P.J., van Oppen, M.J.H., and Lukoschek, V. (2019). Asymmetric dispersal is a critical element of concordance between biophysical dispersal models and spatial genetic structure in Great Barrier Reef corals. Divers. Distrib. *25*, 1684–1696. https://doi.org/10.1111/ddi.12969.

56. Selmoni, O., Lecellier, G., Magalon, H., Vigliola, L., Oury, N., Benzoni, F., Peignon, C., Joost, S., and Berteaux-Lecellier, V. (2021). Seascape genomics reveals candidate molecular targets of heat stress adaptation in three coral species. Mol. Ecol. *30*, 1892–1906. https://doi.org/10.1111/mec.15857.

57. Camp, E.F., Suggett, D.J., Pogoreutz, C., Nitschke, M.R., Houlbreque, F., Hume, B.C.C., Gardner, S.G., Zampighi, M., Rodolfo-Metalpa, R., and Voolstra, C.R. (2020). Corals exhibit distinct patterns of microbial reorganisation to thrive in an extreme inshore environment. Coral Reefs *39*, 701–716. https://doi.org/10.1007/s00338-019-01889-3.

58. Denis, H., Selmoni, O., Gossuin, H., Jauffrais, T., Butler, C.C., Lecellier, G., and Berteaux-Lecellier, V. (2024). Climate adaptive loci revealed by seascape genomics correlate with phenotypic variation in heat tolerance of the coral *Acropora millepora*. Sci. Rep. *14*, 22179. https://doi.org/10.1038/s41598-024-67971-1.

59. Alessi, C., Lemonnier, H., Camp, E.F., Wabete, N., Payri, C., and Rodolfo Metalpa, R. (2024). Algal symbiont diversity in *Acropora muricata* from the extreme reef of Bouraké associated with resistance to coral bleaching. PLoS One *19*, e0296902. https://doi.org/10.1371/journal.pone.0296902.

60. Alvarado-Cerón, V., Muñiz-Castillo, A.I., León-Pech, M.G., Prada, C., and Arias-González, J.E. (2023). A decade of population genetics studies of scleractinian corals: A systematic review. Mar. Environ. Res. *183*, 105781. https://doi.org/10.1016/j.marenvres.2022.105781.

61. Cravatte, S., Kestenare, E., Eldin, G., Ganachaud, A., Lefèvre, J., Marin, F., Menkes, C., and Aucan, J. (2015). Regional circulation around New Caledonia from two decades of observations. J. Mar. Syst. *148*, 249–271. https://doi.org/10.1016/j.jmarsys.2015.03.004.

62. Jokiel, P.L. (1990). Transport of reef corals into the Great Barrier Reef. Nature *347*, 665–667. https://doi.org/10.1038/347665a0.

63. Oury, N., Gélin, P., and Magalon, H. (2020). Cryptic species and genetic connectivity among populations of the coral *Pocillopora damicornis* (Scleractinia) in the tropical southwestern Pacific. Mar. Biol. *167*, 1–15. https://doi.org/10.1007/s00227-020-03757-z.

64. Lukoschek, V., Riginos, C., and van Oppen, M.J.H. (2016). Congruent patterns of connectivity can inform management for broadcast spawning corals on the Great Barrier Reef. Mol. Ecol. *25*, 3065–3080. https://doi.org/10.1111/mec.13649.

65. Marzonie, M.R., Nielsen, J.J.V., Bay, L.K., Bourne, D.G., Nitschke, M.R., Selmoni, O., and Harrison, H.B. (2025). Seascape genomics reveal contrasting population structure in sympatric and congeneric corals across thermal clines. Divers. Distrib. *31*, e70065. https://doi.org/10.1111/ddi.70065.

66. Sully, S., Hodgson, G., and van Woesik, R. (2022). Present and future bright and dark spots for coral reefs through climate change. Glob. Change Biol. *28*, 4509–4522. https://doi.org/10.1111/gcb.16083.

67. Matz, M.V., Treml, E.A., and Haller, B.C. (2020). Estimating the potential for coral adaptation to global warming across the Indo-West Pacific. Glob. Change Biol. *26*, 3473–3481. https://doi.org/10.1111/gcb.15060.

68. Shlesinger, T., and van Woesik, R. (2023). Oceanic differences in coral-bleaching responses to marine heatwaves. Sci. Total Environ. *871*, 162113. https://doi.org/10.1016/j.scitotenv.2023.162113.

69. Scott, C.B., Schott, R., and Matz, M.V. (2024). Cryptic genetic structure of the coral host is the primary driver of holobiont assembly in massive *Porites*. Preprint at bioRxiv. https://doi.org/10.1101/2024.01.09.574877.

70. van Oppen, M.J.H., Bongaerts, P., Frade, P., Peplow, L.M., Boyd, S.E., Nim, H.T., and Bay, L.K. (2018). Adaptation to reef habitats through selection on the coral animal and its associated microbiome. Mol. Ecol. *27*, 2956–2971. https://doi.org/10.1111/mec.14763.

71. Warner, P.A., van Oppen, M.J.H., and Willis, B.L. (2015). Unexpected cryptic species diversity in the widespread coral *Seriatopora hystrix* masks spatial-genetic patterns of connectivity. Mol. Ecol. *24*, 2993–3008. https://doi.org/10.1111/mec.13225.

72. Butler, C.C., Turnham, K.E., Lewis, A.M., Nitschke, M.R., Warner, M.E., Kemp, D.W., Hoegh-Guldberg, O., Fitt, W.K., van Oppen, M.J.H., and

LaJeunesse, T.C. (2023). Formal recognition of host-generalist species of dinoflagellate (*Cladocopium*, Symbiodiniaceae) mutualistic with Indo-Pacific reef corals. J. Phycol. *59*, 698–711. https://doi.org/10.1111/jpy.13340.

73. Slatkin, M. (1987). Gene flow and the geographic structure of natural populations. Science *236*, 787–792. https://doi.org/10.1126/science.3576198.
74. Bridge, T.C.L., Cowman, P.F., Quattrini, A.M., Bonito, V.E., Sinniger, F., Harii, S., Head, C.E.I., Hung, J.Y., Halafihi, T., Rongo, T., et al. (2024). *A tenuis* relationship: traditional taxonomy obscures systematics and biogeography of the '*Acropora tenuis*' (Scleractinia: Acroporidae) species complex. Zool. J. Linn. Soc. *202*, zlad062. https://doi.org/10.1093/zoolinnean/zlad062.
75. Cooper, T.F., Berkelmans, R., Ulstrup, K.E., Weeks, S., Radford, B., Jones, A.M., Doyle, J., Canto, M., O'Leary, R.A., and van Oppen, M.J.H. (2011). Environmental factors controlling the distribution of Symbiodinium harboured by the coral *Acropora millepora* on the Great Barrier Reef. PLoS One *6*, e25536. https://doi.org/10.1371/journal.pone.0025536.
76. Epstein, H.E., Smith, H.A., Cantin, N.E., Mocellin, V.J.L., Torda, G., and van Oppen, M.J.H. (2019). Temporal variation in the microbiome of *Acropora* coral species does not reflect seasonality. Front. Microbiol. *10*, 1775. https://doi.org/10.3389/fmicb.2019.01775.
77. Hoadley, K.D., Pettay, D.T., Lewis, A., Wham, D., Grasso, C., Smith, R., Kemp, D.W., LaJeunesse, T., and Warner, M.E. (2021). Different functional traits among closely related algal symbionts dictate stress endurance for vital Indo-Pacific reef-building corals. Glob. Change Biol. *27*, 5295–5309. https://doi.org/10.1111/gcb.15799.
78. Sampayo, E.M., Franceschinis, L., Hoegh-Guldberg, O., and Dove, S. (2007). Niche partitioning of closely related symbiotic dinoflagellates. Mol. Ecol. *16*, 3721–3733. https://doi.org/10.1111/j.1365-294X.2007.03403.x.
79. Thornhill, D.J., Howells, E.J., Wham, D.C., Steury, T.D., and Santos, S.R. (2017). Population genetics of reef coral endosymbionts (*Symbiodinium*, Dinophyceae). Mol. Ecol. *26*, 2640–2659. https://doi.org/10.1111/mec.14055.
80. Wood, S., Paris, C.B., Ridgwell, A., and Hendy, E.J. (2014). Modelling dispersal and connectivity of broadcast spawning corals at the global scale. Glob. Ecol. Biogeogr. *23*, 1–11. https://doi.org/10.1111/geb.12101.
81. Saint-Amand, A., Lambrechts, J., and Hanert, E. (2023). Biophysical models resolution affects coral connectivity estimates. Sci. Rep. *13*, 9414. https://doi.org/10.1038/s41598-023-36158-5.
82. Marchesiello, P., Lefèvre, J., Vega, A., Couvelard, X., and Menkes, C. (2010). Coastal upwelling, circulation and heat balance around New Caledonia's barrier reef. Mar. Pollut. Bull. *61*, 432–448. https://doi.org/10.1016/j.marpolbul.2010.06.043.
83. Maes, C., and Blanke, B. (2015). Tracking the origins of plastic debris across the Coral Sea: A case study from the Ouvéa Island, New Caledonia. Mar. Pollut. Bull. *97*, 160–168. https://doi.org/10.1016/j.marpolbul.2015.06.022.
84. Hohenlohe, P.A., Funk, W.C., and Rajora, O.P. (2021). Population genomics for wildlife conservation and management. Mol. Ecol. *30*, 62–82. https://doi.org/10.1111/mec.15720.
85. Eddy, T.D., Lam, V.W.Y., Reygondeau, G., Cisneros-Montemayor, A.M., Greer, K., Palomares, M.L.D., Bruno, J.F., Ota, Y., and Cheung, W.W.L. (2021). Global decline in capacity of coral reefs to provide ecosystem services. One Earth *4*, 1278–1285. https://doi.org/10.1016/j.oneear.2021.08.016.
86. Graham, E.M., Baird, A.H., Connolly, S.R., Sewell, M.A., and Willis, B.L. (2013). Rapid declines in metabolism explain extended coral larval longevity. Coral Reefs *32*, 539–549. https://doi.org/10.1007/s00338-012-0999-4.
87. Williamson, D.H., Harrison, H.B., Almany, G.R., Berumen, M.L., Bode, M., Bonin, M.C., Choukroun, S., Doherty, P.J., Frisch, A.J., Saenz-Agudelo, P., et al. (2016). Large-scale, multidirectional larval connectivity among coral reef fish populations in the Great Barrier Reef Marine Park. Mol. Ecol. *25*, 6039–6054. https://doi.org/10.1111/mec.13908.
88. Andréfouët, S., Cabioch, G., Flamand, B., and Pelletier, B. (2009). A reappraisal of the diversity of geomorphological and genetic processes of New Caledonian coral reefs: a synthesis from optical remote sensing, coring and acoustic multibeam observations. Coral Reefs *28*, 691–707. https://doi.org/10.1007/s00338-009-0503-y.
89. Pinsky, M.L., Palumbi, S.R., Andréfouët, S., and Purkis, S.J. (2012). Open and closed seascapes: Where does habitat patchiness create populations with high fractions of self-recruitment? Ecol. Appl. *22*, 1257–1267. https://doi.org/10.1890/11-1240.1.
90. Emslie, M.J., Ceccarelli, D.M., Logan, M., Blandford, M.I., Bray, P., Campili, A., Jonker, M.J., Parker, J.G., Prenzlau, T., and Sinclair-Taylor, T.H. (2024). Changing dynamics of Great Barrier Reef hard coral cover in the Anthropocene. Coral Reefs *43*, 747–762. https://doi.org/10.1007/s00338-024-02498-5.
91. Howells, E.J., Bay, L.K., and Bay, R.A. (2022). Identifying, monitoring, and managing adaptive genetic variation in reef-building corals under rapid climate warming. In Coral Reef Conservation and Restoration in the Omics Age, M.J.H. van Oppen, and M.A. Aranda Lastra, eds. (Springer International Publishing), pp. 55–70. https://doi.org/10.1007/978-3-031-07055-6_4.
92. Quigley, K.M., Ramsby, B., Laffy, P., Harris, J., Mocellin, V.J.L., and Bay, L.K. (2022). Symbioses are restructured by repeated mass coral bleaching. Sci. Adv. *8*, eabq8349. https://doi.org/10.1126/sciadv.abq8349.
93. Turnham, K.E., Lewis, A.M., Kemp, D.W., Warner, M.E., Wham, D.F., Smith, R.T., Hoadley, K., Colin, P.L., Golbuu, Y., and LaJeunesse, T.C. (2025). Limited persistence of the heat-tolerant zooxanthella, *Durusdinium trenchii*, in corals transplanted to a barrier reef where it is rare among natal colonies. Coral Reefs *44*, 555–570. https://doi.org/10.1007/s00338-025-02625-w.
94. Fitzpatrick, S.W., Bradburd, G.S., Kremer, C.T., Salerno, P.E., Angeloni, L.M., and Funk, W.C. (2020). Genomic and fitness consequences of genetic rescue in wild populations. Curr. Biol. *30*, 517–522.e5. https://doi.org/10.1016/j.cub.2019.11.062.
95. Mason, R., Langlais, C., Uribe-Palomino, J., Tonks, M., Coman, F., Choukroun, S., Porobic, J., and Doropoulos, C. (2025). Reef-scale variation in larval supply and settlement: validating dispersal predictions with observations of coral larvae. Estuar. Coast Shelf Sci. *326*, 109506.
96. Mumby, P.J., Mason, R.A.B., and Hock, K. (2021). Reconnecting reef recovery in a world of coral bleaching. Limnol. Oceanogr.: Methods *19*, 702–713. https://doi.org/10.1002/lom3.10455.
97. van Oppen, M.J.H., Gates, R.D., Blackall, L.L., Cantin, N., Chakravarti, L.J., Chan, W.Y., Cormick, C., Crean, A., Damjanovic, K., Epstein, H., et al. (2017). Shifting paradigms in restoration of the world's coral reefs. Glob. Change Biol. *23*, 3437–3448. https://doi.org/10.1111/gcb.13647.
98. Cantin, N., James, N., and Stella, J. (2024). Aerial Surveys of the 2024 Mass Coral Bleaching Event on the Great Barrier Reef (Australian Institute of Marine Science). https://www.aims.gov.au/sites/default/files/2024-04/FINAL-Aerial%20Bleaching%20GBR2024Report_AIMS_Final_15Apr2024_0.pdf.
99. Liu, G., Strong, A.E., and Skirving, W. (2003). Remote sensing of sea surface temperatures during 2002 Barrier Reef coral bleaching. Eos Trans. Am. Geophys. Union *84*, 137–141. https://doi.org/10.1029/2003EO150001.
100. Hersbach, H., Bell, B., Berrisford, P., Biavati, G., Horányi, A., Muñoz Sabater, J., Nicolas, J., Peubey, C., Radu, R., and Rozum, I. (2023). ERA5 hourly data on single levels from 1940 to present. In Climate Data Store (CDS) (Copernicus Climate Change Service [C3S]).
101. Hume, B.C.C., Ziegler, M., Poulain, J., Pochon, X., Romac, S., Boissin, E., De Vargas, C., Planes, S., Wincker, P., and Voolstra, C.R. (2018). An improved primer set and amplification protocol with increased specificity and sensitivity targeting the *Symbiodinium* ITS2 region. PeerJ *6*, e4816. https://doi.org/10.7717/peerj.4816.

102. Bolger, A.M., Lohse, M., and Usadel, B. (2014). Trimmomatic: a flexible trimmer for Illumina sequence data. Bioinformatics *30*, 2114–2120. https://doi.org/10.1093/bioinformatics/btu170.

103. Ewels, P., Magnusson, M., Lundin, S., and Käller, M. (2016). MultiQC: summarize analysis results for multiple tools and samples in a single report. Bioinformatics *32*, 3047–3048. https://doi.org/10.1093/bioinformatics/btw354.

104. Li, H., and Durbin, R. (2010). Fast and accurate long-read alignment with Burrows–Wheeler transform. Bioinformatics *26*, 589–595. https://doi.org/10.1093/bioinformatics/btp698.

105. Li, H., Handsaker, B., Wysoker, A., Fennell, T., Ruan, J., Homer, N., Marth, G., Abecasis, G., and Durbin, R.; 1000 Genome Project Data Processing Subgroup (2009). The sequence alignment/map format and SAMtools. Bioinformatics *25*, 2078–2079. https://doi.org/10.1093/bioinformatics/btp352.

106. Korneliussen, T.S., Albrechtsen, A., and Nielsen, R. (2014). ANGSD: analysis of next generation sequencing data. BMC Bioinformatics *15*, 1–13. https://doi.org/10.1186/s12859-014-0356-4.

107. Van der Auwera, G.A., and O'Connor, B.D. (2020). Genomics in the Cloud: Using Docker, GATK, and WDL in Terra (O'Reilly Media).

108. Danecek, P., Auton, A., Abecasis, G., Albers, C.A., Banks, E., DePristo, M.A., Handsaker, R.E., Lunter, G., Marth, G.T., Sherry, S.T., et al. (2011). The variant call format and VCFtools. Bioinformatics *27*, 2156–2158. https://doi.org/10.1093/bioinformatics/btr330.

109. Purcell, S., Neale, B., Todd-Brown, K., Thomas, L., Ferreira, M.A.R., Bender, D., Maller, J., Sklar, P., De Bakker, P.I.W., Daly, M.J., et al. (2007). PLINK: a tool set for whole-genome association and population-based linkage analyses. Am. J. Hum. Genet. *81*, 559–575. https://doi.org/10.1086/519795.

110. Jombart, T. (2008). adegenet: a R package for the multivariate analysis of genetic markers. Bioinformatics *24*, 1403–1405. https://doi.org/10.1093/bioinformatics/btn129.

111. Alexander, D.H., and Lange, K. (2011). Enhancements to the ADMIXTURE algorithm for individual ancestry estimation. BMC Bioinformatics *12*, 1–6. https://doi.org/10.1186/1471-2105-12-246.

112. Frichot, E., Schoville, S.D., Bouchard, G., and François, O. (2013). Testing for associations between loci and environmental gradients using latent factor mixed models. Mol. Biol. Evol. *30*, 1687–1699. https://doi.org/10.1093/molbev/mst063.

113. Stamatakis, A. (2014). RAxML version 8: a tool for phylogenetic analysis and post-analysis of large phylogenies. Bioinformatics *30*, 1312–1313. https://doi.org/10.1093/bioinformatics/btu033.

114. Korunes, K.L., and Samuk, K. (2021). pixy: Unbiased estimation of nucleotide diversity and divergence in the presence of missing data. Mol. Ecol. Resour. *21*, 1359–1368. https://doi.org/10.1111/1755-0998.13326.

115. Prata, K.E., Riginos, C., Gutenkunst, R.N., Latijnhouwers, K.R.W., Sánchez, J.A., Englebert, N., Hay, K.B., and Bongaerts, P. (2022). Deep connections: Divergence histories with gene flow in mesophotic *Agaricia* corals. Mol. Ecol. *31*, 2511–2527. https://doi.org/10.1111/mec.16391.

116. Hardy, O.J., and Vekemans, X. (2002). SPAGeDi: a versatile computer program to analyse spatial genetic structure at the individual or population levels. Mol. Ecol. Notes *2*, 618–620. https://doi.org/10.1046/j.1471-8286.2002.00305.x.

117. Waples, R.S., and Do, C. (2010). Linkage disequilibrium estimates of contemporary Ne using highly variable genetic markers: a largely untapped resource for applied conservation and evolution. Evol. Appl. *3*, 244–262. https://doi.org/10.1111/j.1752-4571.2009.00104.x.

118. Boyd, J.A., Woodcroft, B.J., and Tyson, G.W. (2018). GraftM: a tool for scalable, phylogenetically informed classification of genes within metagenomes. Nucleic Acids Res. *46*, e59. https://doi.org/10.1093/nar/gky174.

119. Reinert, G., Chew, D., Sun, F., and Waterman, M.S. (2009). Alignment-free sequence comparison (I): statistics and power. J. Comput. Biol. *16*, 1615–1634. https://doi.org/10.1089/cmb.2009.0198.

120. Paradis, E., and Schliep, K. (2019). ape 5.0: an environment for modern phylogenetics and evolutionary analyses in R. Bioinformatics *35*, 526–528. https://doi.org/10.1093/bioinformatics/bty633.

121. Galili, T., Simpson, G., Jefferis, G., Gallotta, M., and Renaudie, J. (2015). Package 'dendextend'. https://cran.r-project.org/web/packages/dendextend/index.html.

122. Hijmans, R.J., Williams, E., Vennes, C., and Hijmans, M.R.J. (2017). Package 'geosphere'. Spherical trigonometry. https://cran.r-project.org/web/packages/geosphere/geosphere.pdf.

123. Dray, S., Blanchet, G., Borcard, D., Guenard, G., Jombart, T., Larocque, G., Legendre, P., Madi, N., Wagner, H.H., and Dray, M.S. (2018). Package 'adespatial'. R package. https://cran.r-project.org/web/packages/adespatial/adespatial.pdf.

124. Oksanen, J., Blanchet, F.G., Kindt, R., Legendre, P., Minchin, P.R., O'Hara, R., Simpson, G.L., Solymos, P., Stevens, M.H.H., and Wagner, H. (2013). Package 'vegan'. Community ecology package. Version 2, pp. 1–295. https://cran.r-project.org/web/packages/vegan/index.html.

125. Wickham, H. (2011). ggplot2. WIREs Computational Stats. *3*, 180–185. https://doi.org/10.1002/wics.147.

126. Cabanettes, F., and Klopp, C. (2018). D-GENIES: dot plot large genomes in an interactive, efficient and simple way. PeerJ *6*, e4958. https://doi.org/10.7717/peerj.4958.

127. Meisner, J., and Albrechtsen, A. (2018). Inferring population structure and admixture proportions in low-depth NGS data. Genetics *210*, 719–731. https://doi.org/10.1534/genetics.118.301336.

128. Wallace, C.C. (1999). Staghorn Corals of the World: A Revision of the Coral Genus *Acropora* (Scleractinia; Astrocoeniina; Acroporidae) Worldwide, with Emphasis on Morphology, Phylogeny and Biogeography (CSIRO Publishing).

129. Denis, H., Bay, L.K., Mocellin, V.J., Naugle, M.S., Lecellier, G., Purcell, S.W., Berteaux-Lecellier, V., and Howells, E.J. (2024). Thermal tolerance traits of individual corals are widely distributed across the Great Barrier Reef. Proc. Biol. Sci. *291*, 20240587.

130. Danecek, P., Bonfield, J.K., Liddle, J., Marshall, J., Ohan, V., Pollard, M.O., Whitwham, A., Keane, T., McCarthy, S.A., Davies, R.M., et al. (2021). Twelve years of SAMtools and BCFtools. GigaScience *10*, giab008. https://doi.org/10.1093/gigascience/giab008.

131. Souter, P., Willis, B., Bay, L., Caley, M., Muirhead, A., and van Oppen, M. (2010). Location and disturbance affect population genetic structure in four coral species of the genus *Acropora* on the Great Barrier Reef. Mar. Ecol. Prog. Ser. *416*, 35–45. https://doi.org/10.3354/meps08740.

132. Yang, J., Benyamin, B., McEvoy, B.P., Gordon, S., Henders, A.K., Nyholt, D.R., Madden, P.A., Heath, A.C., Martin, N.G., Montgomery, G.W., et al. (2010). Common SNPs explain a large proportion of the heritability for human height. Nat. Genet. *42*, 565–569. https://doi.org/10.1038/ng.608.

133. Schmidt, T.L., Jasper, M.E., Weeks, A.R., and Hoffmann, A.A. (2021). Unbiased population heterozygosity estimates from genome-wide sequence data. Methods Ecol. Evol. *12*, 1888–1898. https://doi.org/10.1111/2041-210X.13659.

134. Lou, R.N., and Therkildsen, N.O. (2022). Batch effects in population genomic studies with low-coverage whole genome sequencing data: Causes, detection and mitigation. Mol. Ecol. Resour. *22*, 1678–1692. https://doi.org/10.1111/1755-0998.13559.

135. Fenner, D., and Muir, P. (2008). Species of reef corals observed in northwestern lagoon of Grande Terre, New Caledonia. In A Rapid Marine Biodiversity Assessment of the Coral Reefs of the Northwest Lagoon, between Koumac and Yandé (Conservation International), p. 149.

136. Weir, B.S., and Cockerham, C.C. (1984). Estimating F-statistics for the analysis of population structure. Evolution *38*, 1358–1370.

137. Frichot, E., Mathieu, F., Trouillon, T., Bouchard, G., and François, O. (2014). Fast and efficient estimation of individual ancestry coefficients. Genetics *196*, 973–983. https://doi.org/10.1534/genetics.113.160572.

138. Hemstrom, W., Grummer, J.A., Luikart, G., and Christie, M.R. (2024). Next-generation data filtering in the genomics era. Nat. Rev. Genet. *25*, 750–767. https://doi.org/10.1038/s41576-024-00738-6.

139. Nand, A., Zhan, Y., Salazar, O.R., Aranda, M., Voolstra, C.R., and Dekker, J. (2021). Genetic and spatial organization of the unusual chromosomes of the dinoflagellate *Symbiodinium microadriaticum*. Nat. Genet. *53*, 618–629. https://doi.org/10.1038/s41588-021-00841-y.

140. Shoguchi, E., Shinzato, C., Kawashima, T., Gyoja, F., Mungpakdee, S., Koyanagi, R., Takeuchi, T., Hisata, K., Tanaka, M., Fujiwara, M., et al. (2013). Draft assembly of the *Symbiodinium minutum* nuclear genome reveals dinoflagellate gene structure. Curr. Biol. *23*, 1399–1408. https://doi.org/10.1016/j.cub.2013.05.062.

141. Chen, Y., Shah, S., Dougan, K.E., van Oppen, M.J.H., Bhattacharya, D., and Chan, C.X. (2022). Improved *Cladocopium goreaui* genome assembly reveals features of a facultative coral symbiont and the complex evolutionary history of dinoflagellate genes. Microorganisms *10*, 1662. https://doi.org/10.3390/microorganisms10081662.

142. Dougan, K.E., Bellantuono, A.J., Kahlke, T., Abbriano, R.M., Chen, Y., Shah, S., Granados-Cifuentes, C., van Oppen, M.J.H., Bhattacharya, D., Suggett, D.J., et al. (2024). Whole-genome duplication in an algal symbiont bolsters coral heat tolerance. Sci. Adv. *10*, eadn2218. https://doi.org/10.1126/sciadv.adn2218.

143. Shah, S., Dougan, K.E., Chen, Y., Lo, R., Laird, G., Fortuin, M.D.A., Rai, S.K., Murigneux, V., Bellantuono, A.J., Rodriguez-Lanetty, M., et al. (2024). Massive genome reduction predates the divergence of Symbiodiniaceae dinoflagellates. ISME J. *18*, wrae059. https://doi.org/10.1093/ismejo/wrae059.

144. Li, T., Yu, L., Song, B., Song, Y., Li, L., Lin, X., and Lin, S. (2020). Genome improvement and core gene set refinement of *Fugacium kawagutii*. Microorganisms *8*, 102. https://doi.org/10.3390/microorganisms8010102.

145. Armstrong, E.J., Lê-Hoang, J., Carradec, Q., Aury, J.-M., Noel, B., Hume, B.C.C., Voolstra, C.R., Poulain, J., Belser, C., Paz-García, D.A., et al. (2023). Host transcriptomic plasticity and photosymbiotic fidelity underpin *Pocillopora* acclimatization across thermal regimes in the Pacific Ocean. Nat. Commun. *14*, 3056. https://doi.org/10.1038/s41467-023-38610-6.

146. González-Pech, R.A., Stephens, T.G., Chen, Y., Mohamed, A.R., Cheng, Y., Shah, S., Dougan, K.E., Fortuin, M.D.A., Lagorce, R., Burt, D.W., et al. (2021). Comparison of 15 dinoflagellate genomes reveals extensive sequence and structural divergence in family Symbiodiniaceae and genus *Symbiodinium*. BMC Biol. *19*, 1–22. https://doi.org/10.1186/s12915-021-00994-6.

147. Borcard, D., and Legendre, P. (2002). All-scale spatial analysis of ecological data by means of principal coordinates of neighbour matrices. Ecol. Modell. *153*, 51–68. https://doi.org/10.1016/S0304-3800(01)00501-4.

148. Fanton d'Andon, O., Mangin, A., Lavender, S., Antoine, D., Maritorena, S., Morel, A., Barrot, G., Demaria, J., and Pinnock, S. (2009). GlobColour-the European Service for Ocean Colour. In Proceedings of the 2009 IEEE International Geoscience & Remote Sensing Symposium (IGARSS).

149. Sopniewski, J., and Catullo, R.A. (2024). Estimates of heterozygosity from single nucleotide polymorphism markers are context-dependent and often wrong. Mol. Ecol. Resour. *24*, e13947. https://doi.org/10.1111/1755-0998.13947.

150. Rousset. (1999). Genetic differentiation between individuals. J. Evol. Biol. *13*, 58–62. https://doi.org/10.1046/j.1420-9101.2000.00137.x.

151. Hardy, O.J., and Vekemans, X. (1999). Isolation by distance in a continuous population: reconciliation between spatial autocorrelation analysis and population genetics models. Heredity *83*, 145–154. https://doi.org/10.1046/j.1365-2540.1999.00558.x.

152. Neel, M.C., McKelvey, K., Ryman, N., Lloyd, M.W., Short Bull, R., Allendorf, F.W., Schwartz, M.K., and Waples, R.S. (2013). Estimation of effective population size in continuously distributed populations: there goes the neighborhood. Heredity *111*, 189–199. https://doi.org/10.1038/hdy.2013.37.

153. Waples, R.S., and Do, C. (2008). LDNE: a program for estimating effective population size from data on linkage disequilibrium. Mol. Ecol. Resour. *8*, 753–756. https://doi.org/10.1111/j.1755-0998.2007.02061.x.

154. Legendre, P., and Anderson, M.J. (1999). Distance-based redundancy analysis: testing multispecies responses in multifactorial ecological experiments. Ecol. Monogr. *69*, 1–24. https://doi.org/10.1890/0012-9615(1999)069[0001:DBRATM]2.0.CO;2.

155. Capblancq, T., and Forester, B.R. (2021). Redundancy analysis: A Swiss Army Knife for landscape genomics. Methods Ecol. Evol. *12*, 2298–2309. https://doi.org/10.1111/2041-210X.13722.

STAR★METHODS

KEY RESOURCES TABLE

REAGENT or RESOURCE	SOURCE	IDENTIFIER
Chemicals, peptides, and recombinant proteins		
DNeasy Blood & Tissue Kit	Qiagen	Cat#69504
Lotus DNA Library Prep Kit	Integrated DNA Technologies (IDT)	Cat#10009819
Truseq Nano DNA Kit	Illumina	Cat#20015965
Herculase II Fusion DNA Polymerase Nextera XT Index V2 Kit	Agilent Technologies	Cat#600675
Deposited data		
Raw sequence data for the whole genome sequencing (WGS) of GBR samples	This paper	NCBI:PRJNA1390968
Raw sequence data for the whole genome sequencing (WGS) of NC samples	This paper	NCBI:PRJNA1357023
ITS2 rRNA amplicon sequencing data	This paper	Symportal:20250122T050733 _denishu1
SymPortal	Hume et al.[44]	https://symportal.org/
NOAA Coral Reef Watch's (CRW) V3.1 Daily Global 5km Satellite Coral Bleaching Heat Stress product	Liu et al.[99]	https://coralreefwatch.noaa.gov/product/5km/
ERA5	Hersbach et al.[100]	DOI:10.24381/cds.adbb2d47
GlobColour, ESA	Copernicus Marine Service	DOI:10.48670/moi-00279
GADM Administrative boundaries, V4.1	Global Administrative Areas	https://gadm.org/
Oligonucleotides		
ITS2 primers; SYM_VAR_5.8S; F: 5'-GAATTGCAGAACTCCGTGAACC-3′	Hume et al.[101]	N/A
ITS2 primers; SYM_VAR_REV; R: 5'-CGGGTTCWCTTGTYTGACTTCATGC-3′	Hume et al.[101]	N/A
Software and algorithms		
Trimmomatic v0.39	Bolger et al.[102]	http://www.usadellab.org/cms/index.php?page=trimmomatic; RRID: SCR_011848
FastQC v0.12.1	N/A	https://www.bioinformatics.babraham.ac.uk/projects/fastqc/; RRID: SCR_014583
MultiQC v1.21	Ewels et al.[103]	http://multiqc.info/; RRID: SCR_014982
Burrow-Wheeler Aligner v0.7.17	Li and Durbin[104]	https://bio-bwa.sourceforge.net/; RRID: SCR_010910
Samtools v1.20 / bcftools v1.20	Li et al.[105]	https://github.com/samtools/; RRID: SCR_002105
Picard v3.1.1	Broad Institute	http://broadinstitute.github.io/picard/; RRID: SCR_006525
ANGSD v0.940	Korneliussen et al.[106]	https://github.com/ANGSD/angsd; RRID: SCR_021865
GATK v4.5.0.0	Van der Auwera and O'Connor[107]	https://software.broadinstitute.org/gatk/; RRID: SCR_001876
vcftools v0.1.17	Danecek et al.[108]	https://vcftools.github.io/; RRID: SCR_001235
plink v1.90b7.2	Purcell et al.[109]	https://www.cog-genomics.org/plink/; RRID: SCR_001757
adegenet v2.1.10	Jombart et al.[110]	https://cran.r-project.org/web/packages/adegenet/; RRID: SCR_000825
ADMIXTURE v1.3.0	Alexander and Lange[111]	https://dalexander.github.io/admixture/; RRID: SCR_001263
LEA v3.14.0	Frichot et al.[112]	https://github.com/bcm-uga/LEA

(*Continued on next page*)

Continued

REAGENT or RESOURCE	SOURCE	IDENTIFIER
vcf2phylip.py	N/A	https://github.com/edgardomortiz/vcf2phylip; DOI:10.5281/zenodo.2540861
RAxML	Stamatakis[113]	https://github.com/stamatak/standard-RAxML; RRID: SCR_006086
pixy v1.2.10	Korunes and Samuk[114]	https://pixy.readthedocs.io/; DOI: 10.1111/1755-0998.13326
∂a∂i v2.3.3	Gutenkunst et al.[29]	https://dadi.readthedocs.io/
vcf_minrep_filter.py	N/A	https://github.com/pimbongaerts/radseq/blob/master/vcf_minrep_filter.py
∂a∂i workflow	Prata et al.[115]	https://github.com/kepra3/kp_dadi
spagedi v1.5	Hardy and Vekemans[116]	https://ebe.ulb.ac.be/ebe/SPAGeDi.html
LDN_e v2.1	Waples and Do[117]	https://ldne.software.informer.com/download/
Symbiodiniaceae analysis workflow	Ishida et al.[49]	https://github.com/hisatakeishida/Symb-SHIN
graftM v0.15.1	Boyd et al.[118]	https://github.com/geronimp/graftM
jellyfish v1.1.12	N/A	https://github.com/gmarcais/Jellyfish; RRID: SCR_005491
d2ssect	Reinert et al.[119]	https://github.com/bakeronit/d2ssect
ape v5.8.1	Paradis and Schliep[120]	https://cran.r-project.org/web/packages/ape/index.html
dendextend	Galili et al.[121]	https://talgalili.github.io/dendextend/; RRID: SCR_026116
geosphere	Hijmans et al.[122]	https://cran.r-project.org/web/packages/geosphere/
adespatial	Dray et al.[123]	https://cran.r-project.org/web/packages/adespatial/
vegan	Oksanen et al.[124]	http://cran.r-project.org/web/packages/vegan/; RRID: SCR_011950
BBMap v35.85 reformat.sh	N/A	https://sourceforge.net/projects/bbmap/; RRID: SCR_016965
R v4.0.4	R Core Team	http://www.r-project.org/; RRID: SCR_001905
ggplot2	Wickham[125]	https://cran.r-project.org/web/packages/ggplot2/; RRID: SCR_014601
D-GENIES	Cabanettes and Klopp[126]	http://dgenies.toulouse.inra.fr/; RRID: SCR_018967
PCAngsd v1.21	Meisner and Albrechtsen[127]	https://github.com/Rosemeis/pcangsd; RRID: SCR_026956

EXPERIMENTAL MODEL AND STUDY PARTICIPANT DETAILS

Study sites and sample collection

A. cf. *spathulata* was sampled from the east coast of Australia to the west coast of New Caledonia and across a 10 ° latitudinal gradient (Table S1). Colonies were identified in the field based on their morphological similarity to the nominal species, and prior taxonomic work on the Great Barrier Reef (GBR).[128] Field identification focused on colonies with a compact corymbose morphology, distinctive labellate (scale-like) radial corallites, and thick branches. The latter character was primarily used to distinguish *A.* cf. *spathulata* colonies from the closely related *A. millepora*, which has finer branches.[128] The lack of publicly available genomic data from *A. spathulata* topotypes from the Solomon Islands population prevents a genomic-based verification of their taxonomic status as populations of the same species or currently synonymized species, hence the *cf.* qualifier used here. The first batch of samples consisted of 831 colonies collected across 15 reefs of the GBR (n = 40–60 per reef; Figure 1) between 28 February and 26 March 2022 (GBRMPA permit G21/45166.1) as described by Denis et al.[129] The second batch comprised 323 colonies collected across 14 reefs of the western coast of New Caledonia (NC) and atolls of the Chesterfield-Bellona (CB) plateau located in the Coral Sea (n = 4–25 per reef) between 26 June and 28 September 2023 (New Caledonia Natural Park of the Coral Sea permit 2023-1503/GNC, South Province permit 4508- 2022/ARR/DDDT and North Province permit 609011). At each reef, small fragments (< 1 cm^3) were collected on SCUBA from coral colonies originating from one or two sites (covering 50–4200 m^2) and immediately stored in 80–100% ethanol for DNA extraction. Depending on reef site geomorphology, colonies were collected from upper reef slopes, fringing reefs, inner barrier reefs or reef flats at an average depth of 0.6 m (−0.7 m to 5.6 m relative to the lowest astronomical tide, Table S1). Geographic coordinates were recorded for each colony by carrying a GPS in tow on a surface float (except at NC and CB reefs), and whole colony photographs and macrophotographs were taken of each colony using an Olympus TG-6. The occurrence of clones was minimized by avoiding sampling neighboring colonies of similar pigmentation.

METHOD DETAILS

DNA extraction and sequencing

Coral fragments from 1,154 colonies were used for DNA extraction and 1,144 high quality DNA samples were used for library preparation and whole genome sequencing (Table S2). While extraction and sequencing of the GBR and New Caledonia samples were conducted at different facilities, similar extraction and library preparation kits and sequencing platforms were used in order to minimize batch effects. In addition, a subset of 23 technical replicates pairs from the GBR was extracted and sequenced alongside both batches to control for such effects (see STAR Methods, testing for batch effects). In both cases, total DNA was extracted from coral tissue slurry (tissue and skeleton) using the DNeasy Blood and Tissue Kit (Qiagen, Hilden, Germany) following manufacturer's instruction, including an RNAse digestion step for GBR samples (30 min at room temperature). For GBR samples, sequencing libraries were prepared using the Lotus DNA Library Prep Kit for NGS (10 ng of input DNA, 8 PCR cycles) and sequenced on the Illumina NovaSeq 6000 platform (200 cycles; 150 bp paired end reads; targeting 10X coverage; Azenta Life Sciences, CSIRO). For New Caledonia samples, the libraries were prepared using the Truseq Nano DNA kit (200 ng of input DNA, 8 PCR cycles) and sequenced on the Illumina NovaSeq X platform (300 cycles; 150 bp paired end reads; targeting 10X coverage; Macrogen, Korea).

Genomic data pre-variant processing and filtering

The bioinformatic pipeline used to process, filter, and analyze the genomic data is outlined in Figure S7A. The dataset consisted of the 1,144 sequenced individuals with technical replicates (n = 25; see STAR Methods, testing for batch effects) and *Acropora millepora* samples used as outgroups (n = 13). Pre-variant filtering steps are summarized in Table S2. Adapter removal and read quality trimming was conducted using *Trimmomatic* v0.39[102] with a 4 bp sliding window, a minimum Phred score quality of 20, and a minimum read length of 50 bp. Leading and trailing low quality bases were removed (LEADING:3, TRAILING:3) and adapter sequences were removed using the Illuminaclip option in 'palindrome mode' (2:30:10:4). Sample quality was confirmed using *FastQC* v0.12.1 (http://www.bioinformatics.bbsrc.ac.uk/projects/fastqc) and *MultiQC* v1.21.[103] Filtered reads were then aligned to the *Acropora millepora* reference genome v3 assembly (unpublished upgrade from GCA_013753865.1_Amil_v2.1; see choice of reference genome) using the *Burrow-Wheeler Aligner* v0.7.17[104] and the *MEM* algorithm at default settings. SAM files were converted to indexed and sorted BAM files using *Samtools* v1.20[105,130] and PCR duplicates were marked and removed using *Picard* v3.1.1 (VALIDATION_STRINGENCY=LENIENT; http://broadinstitute.github.io/picard/). After removing samples that failed sequencing and samples with unexpectedly low percentage of mapped reads (< 80%; possibly indicative of mis-identified taxa) or number of mapped reads (< 10M), 1,132 BAM files were retained (Figures S7B and S7C). To provide an initial evaluation of population structure across the study system and pinpoint potential clones and taxa misidentification, this dataset was analyzed alongside outgroup samples using a genotype likelihood framework in *ANGSD* v0.940[106] (see STAR Methods, host population genomic using genotype likelihoods). Four samples from the GBR belonging to *A. millepora* and 23 samples from a distinct unknown genetic cluster from NC were removed from further analyses.

Choice of reference genome

Cleaned reads were aligned to *Acropora millepora* v3 reference genome (unpublished upgrade from GCA_013753865.1_Amil_v2.1). This reference was chosen as *A. millepora* is a very close taxa to *A.* cf. *spathulata*, both phylogenetically and morphologically[131] and had a curated chromosome-scale reference genome at the time analyses were performed unlike *A.* cf. *spathulata*. Since initial analyses were performed, two *A.* cf. *spathulata* reference genomes have become available on NCBI Genbank (one chromosome scale; GCA_964019555.1 and one contig-scale; GCA_031770025.1). However, alignment of both reference genomes using D-GENIES[126] revealed a moderate macrosynteny between the two *A.* cf. *spathulata* reference genomes and limited microsynteny with less than 5% of the reference genomes showing > 75% identity. For comparison, these levels of identity or on the same order of magnitude than between two different species: *A. tenuis* with *A. millepora*[50] which suggests that better curation of these references might be needed. In addition, preliminary tests mapping reads from our samples to the contig-scale *A. spathulala* reference (GCA_031770025.1) and *A. millepora v3* showed only a < 0.3% difference in mapping rates between them. The better quality, curation and assembly scale of *A. millepora v3* reference genome thus made it a preferable choice for our analyses.

SNP calling, clone identification and filtering

Indexed, duplicate-free BAM files were used to call variants and genotypes from a total of 1,105 remaining samples using *GATK* v4.5.0.0 'Germline short variant discovery best practice' workflow.[107] Variant calling was first performed per sample, focusing only on reads mapping to the 14 reference chromosomes, using the *HaplotypeCaller* tool that performs *de novo* assembly of haplotypes in active regions. Individual 'gvcf' files were then consolidated per chromosome using *GenomicDBimport* and used for joint genotyping using *GenotypeGVCFs* tool. *GatherVCFs* and *SelectVariants* tools were used to combine chromosome files in a single variant call format (VCF) file and separate SNPs from INDELs and monomorphic sites. The SNPs VCF file was preliminarily filtered using *GATK VariantFiltration* tool following GATK stringent filtering best practices (QD > 2, FS < 50, MQ > 40, MQRankSum > -12.5, ReadPosRankSum > -8, SOR < 3, GQ > 20) and 17 individuals with high missingness (> 85%) were discarded (Figure S7D). Previously identified putative clonal colonies were confirmed and filtered to retain only one colony with the lowest missingness per clonal group (see STAR Methods, clones and related individuals' identification, Table S3, and Figures S3E–S3H).

Testing for batch effects

For logistical and legal reasons, samples collected in Australia and New Caledonia were processed for DNA extraction, library preparation and sequencing at different facilities. While we used similar DNA extraction kits, library preparation kits and sequencing platform to minimize batch effects in our dataset, a subset of 23 GBR samples were extracted and sequenced separately at both facilities to validate the absence of strong batch effects. Following the different data processing steps described in above, 17 pairs of samples passed filtering steps and were used to assess the presence of batch effects using 'hard called' variants. First, a relatedness matrix was generated in *vcftools* v0.1.17 using the method of Yang et al.[132] from these 17 pairs of technical replicates across batches, 2 pairs of technical replicates within the same GBR batch and 100 additional random samples. Each pair of replicates were correctly grouped together based on relatedness, irrespective of the batch in which they were sequenced (Figure S8A). Second, a PCA was conducted on 130,344 SNPs (MAF > 0.01, missingness < 20%) from these 17 pairs of technical replicates using the *glPca* function in R package *adegenet* v2.1.10,[110] as described in the host population genomics analyses section below. The PCA correctly separated GBR samples in the two previously described genomic clusters, rather than by batch (Figure S8B). Third, we computed individual autosomal heterozygosity for these 17 pairs of technical replicates using *vcftools* v0.1.17 and *bcftools* v1.20. Autosomal heterozygosity was computed using 0% missing data (2,715 SNPs) following recommendations from Schmidt et al.[133] This was done because different factors such as different levels of DNA degradation leading to base transition can alter heterozygosity estimates between batches.[134] A Welch two-sample t-test found no significant differences in heterozygosity between batches (Figure S8C). Overall, these results confirm the absence of strong batch effects in our dataset. While slight differences between samples extracted and sequenced separately are to be expected, the genetic patterns described in this study are unlikely to be an artifact of batch effects.

Host population genomic using genotype likelihoods

To get an initial impression of the population structure across our study system we analyzed coral samples genomic data with a genotype likelihood framework in ANGSD v0.940.[106] The dataset comprised the 1,132 putative *A.* cf. *spathulata* samples and validated *A.millepora* (n = 13) samples used as outgroups, processed using the same pipeline. Polymorphic sites were filtered to retain only those with mapping quality > 30, base quality > 30, coverage $\geq$ 3 paired-end reads in $\geq$95% of individuals, and sites mapping to 14 assembled chromosomes. Genotype likelihoods were inferred using the Samtools model to estimate major and minor alleles frequencies assuming biallelic sites (-doMaf = 2) and considered only polymorphic sites with a likelihood ratio test p-value < 0.000001.

A. cf. *spathulata* distribution is currently recognized to encompass the GBR. A first subset of the dataset including 864 GBR individuals was used to pinpoint potential taxon misidentification. To that end, polymorphic sites with minor allele frequency (MAF) > 0.05 were used to compute a covariance matrix and perform a principal component analysis (PCA) in PCAngsd v1.21.[127] Bayesian hierarchical clustering admixture analyses was also performed in PCAngsd with the 'admix' option assuming 2–5 ancestral populations. Both analyses revealed two major genomic clusters geographically separated between the central/north and south GBR. In both analyses, 4 samples were also detected as being *A. millepora* colonies that were mis-identified in the field and were discarded in further analyses (Figure S9A).

A. cf. *spathulata* has been less often identified and studied in New Caledonia despite being reported to occur in the Western Lagoon of the main island 'Grande Terre'.[135] Prior work targeting *A. millepora* has also revealed several genetic clusters that could actually consist of the two species or other related taxa.[56] In the field, colonies most closely matching *A.* cf. *spathulata* morphology from the Great Barrier Reef were targeted. We further assessed how these colonies related to the GBR *A.* cf. *spathulata* and *A. millepora* by repeating the same PCA and Ancestry analyses using a dataset of 1,041 colonies from the Central/North and South GBR, New Caledonia as well as *A. millepora* from the central GBR (Figure S9B). These analyses suggested that colonies collected in New Caledonia were indeed most closely related to the GBR *A.* cf. *spathulata* than the GBR *A. millepora*. Colonies sampled in the western coast of New Caledonia (NC) and the Chesterfields-Bellona plateau (CB) formed two genetically distinct groups. In addition, a small subset of 23 samples from the southern west coast of New Caledonia clustered separately from the rest, presumably originating from an undersampled genetically distinct group that appears closer to the GBR *A. millepora*.

Validation of differentiation from *A. millepora*

To confirm genetic differentiation of previously described groups, an even subset of 11 individuals for each of the 6 groups (*GBR A. millepora*, Central/North GBR *A.* cf. *spathulata*, South GBR *A.* cf. *spathulata*, NC Cluster 1, NC Cluster 2 and CB) was used for SNPs and variant calling using the same GATK pipeline and filtering steps as described above. The resulting vcf file was used to compute Pairwise F_{st} between each group using the Weir and Cockerham method[136] in *vcftools*, and used to perform a PCA with the *glPca* function from R package *adegenet* v2.1.10.[110] These analyses confirmed that all sampled taxa in this study were most closely related to the GBR *A.* cf. *spathulata* (Figures S9C and S9D). The PCA analysis also confirmed the presence of two genetically distinct groups in the western coast of New Caledonia. Due to its low sample size, the under sampled Cluster 2 was discarded from further analyses to focus on the predominant Cluster 1.

Clones and related individuals' identification

Clonemates and related individuals were identified in the dataset using two methods. First, identity-by-state (IBS) matrices were generated in *ANGSD* using the *-doIBS* function from the set of filtered polymorphic sites. Second, relatedness matrices were generated from hard called variants (20% missingness) in *vcftools* using the method of Yang et al.[132] In both cases, matrices were computed and clonemates identified separately for each of the four genetic groups (NC, CB, South GBR and Central/North GBR).

Colonies' genetic similarity was compared to the overall background similarity as well as the similarity of technical replicates to infer pairs or groups of clonemates. Both IBS and relatedness agreed for all pairs or groups of clones. Using a conservative relatedness threshold of 0.2, there were 11, 17, 3 and 6 groups of clones or related individuals for the Central/North GBR, the South GBR, NC and CB respectively (Figures S3E–S3H). The number of putative clones and highly related individuals was particularly high in the Southern GBR but we could not confirm if this was due to higher inbreeding rates at these locations or an artifact of the sampling scheme, as colonies were sampled randomly by different groups of divers between locations. All related individuals identified using a conservative threshold were filtered prior to final population structure, demographic and isolation by distance analyses to retain one individual with the lowest missingness per group.

Host population genomics analyses

To confirm the absence of strong batch effects that could confound population structure, a subset of 23 pairs of technical replicates was sequenced along both GBR and NC samples (see STAR Methods, testing for batch effects and Figure S8). After exclusion of natural clones and technical replicates, a final set of 999 individuals was used for host population genetic analyses. A first dataset of unlinked SNPs was created to investigate population structure and phylogenetic relationship between populations of the Western Pacific, retaining only bi-allelic SNPs with a minimum mean locus depth of 5 and a maximum of 15, a minor allele frequency (MAF) > 0.05 and a locus missingness < 20% with *vcftools* v0.1.17.[108] In addition, SNPs in linkage disequilibrium with a pairwise $r^2 > 0.2$ were removed using *plink* v1.90b7.2[109] ("Dataset 1", Table S4) because we were interested in identifying neutral population structure patterns that occur throughout the genome. To identify genetically distinct groups of individuals, we performed a principal component analysis (PCA) with the *glPca* function from R package *adegenet* v2.1.10.[110] We then estimated individual ancestry proportion using ADMIXTURE v1.3.0.[111] The optimal number of ancestral populations ($K = 4$) was determined using the cross-validation method implemented in ADMIXTURE (Figure S2A). To complement these analyses, we estimated individual ancestry proportion using sparse Non-negative Matrix Factorization (sNMF) with the R package *LEA* v3.14.0.[137] The optimal number of ancestral populations was estimated using the minimum average cross-entropy value over five repetitions with $\alpha = 100$ (Figure S2C). To investigate potential fine-scale genetic structure, we repeated the ADMIXTURE analysis within each major population using $K = 2$ (Figures S3A–S3D). Following Hemstrom et al.[138] best practices, these analyses were also conducted using variable stringency MAF (MAF > 0.01 and MAF > 0.05) and missingness thresholds (5%, 10%, 20% and 50%).

Finally, we used a subset of individuals with the highest ancestral assignment in ADMIXTURE (200 colonies, 50 colonies per population) and built an individual-based Maximum Likelihood phylogenetic tree using RAxML.[113] To build the tree, the VCF file was converted to the Phylip format using *vcf2phylip.py* script (https://github.com/edgardomortiz/vcf2phylip) and raxmlHPC-PTHREADS was run with a GTRGAMMA model and 100 bootstrap replicates.

Demographic modeling

To investigate the evolutionary history and connectivity of these populations, a subset of Dataset 2 comprising 120 colonies (30 colonies per population, showing >95% admixture cluster assignment) was used to conduct demographic modeling analyses in *∂a∂i* v2.3.3.[29] This dataset was further filtered to retain SNPs with a minimum allele count (MAC) of 3 to minimize the effect of sequencing errors. SNPs showing a deviation from HWE (p-value < 0.0001) were also removed as we observed an excess in heterozygosity creating a peak in the SFS at 0.5 haplotype frequency, potentially due to gene duplication, paralogous loci or balancing selection. Finally, a second round of filtration to ensure < 20% missingness within each population was performed using *vcf_minrep_filter.py* script (https://github.com/pimbongaerts/radseq, "Dataset 3", Table S4). VCF files were created for each population pair (n=6) and analyzed using a custom workflow to estimate effective population sizes, divergence time and migration rates between populations (https://github.com/kepra3/kp_dadi).

We computed joint-allelic frequency spectrums (JAFS) for each pair using the subsample method to account for missing data, and masking singletons and doubletons to minimize the effect of sequencing errors or somatic mutations. We initially tested three scenarios: divergence in isolation, divergence with asymmetrical migration and ancestral asymmetrical migration (Figure S4A). We optimized the models' parameters to best fit the observed JAFS (Figure S4B). To avoid getting stuck in local optima, optimization was performed by exploring the parameter space in three stages: first with three-fold, then two-fold, and finally one-fold perturbations of the starting parameters, based on the previously optimized peak values (>100 runs per stage). The final set of parameters was chosen when appearing several times with 1-fold perturbation from different initial values. To get confidence intervals for these parameters, 100 bootstraps were created for each pair by resampling genomic contigs. Optimization runs (n=50) were performed for each bootstrap and model, using 1-fold perturbations starting from previously optimized parameters. For each bootstrap replicate, delta-AIC values were computed between models, and the mean delta-AIC across replicates was used to identify the best-fitting model for each population pair (Figure S4C). Optimized parameters from the best-fitting model (divergence with asymmetrical migration) were used to calculate 95% credible intervals, after excluding bootstrap replicates within the lowest 10% likelihood quantile.

Finally, we converted parameter values obtained in *∂a∂i* (θ, ν_{1dadi}, ν_{2dadi}, M_{12dadi}, M_{12dadi} and T_{dadi}) into physical units: divergence time in years, effective population sizes in number of individuals and gene flow between taxa in number of migrants per generation. To do so we first calculated the effective sequence length for each pair as:

$$L = \frac{SNP_{dadi}}{SNP_{detected}} \times N_{sites}$$

where SNP_{dadi} is the number of SNPs used to construct the JAFS from the specific pair, $SNP_{detected}$ is the number of SNPs originally detected before filtration, and N_{sites} is the number of sites obtained from GATK pipeline (including SNPs, INDELs and monomorphic sites). Next, we computed the ancestral population size (N_{ref}) and the effective population sizes ν_1 and ν_2 in number of individuals, the divergence time (T) in years, migration rates in fraction of migrant individuals at each generation (m_{12}; from Population 2 to Population 1 and m_{21}; from Population 1 to Population 2) and rates of gene flow in number of individuals per generation (M_{12} and M_{21}), using the following formulas:

$$N_{ref} = \frac{\theta}{4 \times \mu \times L}$$

$$T = 2 \times T_{gen} \times N_{ref} \times T_{dadi}$$

$$\nu_1 = \nu_{1dadi} \times N_{ref}$$

$$\nu_2 = \nu_{2dadi} \times N_{ref}$$

$$m_{12} = \frac{M_{12dadi}}{2 \times N_{ref}}$$

$$m_{21} = \frac{M_{21dadi}}{2 \times N_{ref}}$$

$$M_{12} = m_{12} \times \nu_1$$

$$M_{21} = m_{21} \times \nu_2$$

We used a mutation rate μ of 1.2×10^{-8} mutations per base per generation, previously estimated for *Acropora* corals[32] and a generation time T_{gen} of 5 years following the assumptions of Matz et al.[30] on generation times of *A. millepora*.

Symbiodiniaceae community analyses

We used genomic reads from 1,088 *A.* cf. *spathulata* holobionts to characterize symbiont community composition and diversity across our study area, adopting the approach by Ishida et al.,[49] available at https://github.com/hisatakeishida/Symb-SHIN. Genomic reads not mapping to the host reference genome (i.e. non-coral reads) were first re-aligned to several reference genomes of Symbiodiniaceae using the Burrow-Wheeler Aligner v0.7.17[104] and the MEM algorithm (*bwa-mem*) at default setting, with one reference per genus (*Symbiodinium microadriaticum* CCMP2467,[139] *Breviolum minutum* Mf1.05b,[140] *Cladocopium proliferum* SCF055-01,[141] *Durusdinium trenchii* CCMP2556,[142] *Effrenium voratum* RCC1521[143] and *Fugacium kawagutii* CCMP2468[144]).

For the first-pass analysis of the symbiont community composition, we retrieved and classified ITS2 sequences present in the samples using *graftM* v0.15.1.[118] All ITS2 sequence variants were classified as belonging to genus *Cladocopium*. To improve intra-specific taxonomic resolution, we also analysed *psbA*^{ncr} sequences among the samples. We retrieved *psbA*^{ncr} sequences by mapping reads to a custom *psbA*^{ncr} reference database using *bwa-mem*. We then followed Armstrong et al.[145] to retain only reads that aligned in full length (100% cover) at >90% identity, and used number of uniquely mapped reads as proxy for abundance.

To capture genetic diversity of symbionts directly using whole-genome sequencing data not restricted to selected marker genes, we adopted a *k*-mer-based alignment-free approach, following earlier studies.[32,49] The *k*-mers in each sample were first enumerated using *jellyfish* v1.1.12 (https://github.com/gmarcais/Jellyfish) at $k = 21$, yielding a 21-mer profile following previous studies.[146] Pairwise distance between samples was computed from these profiles using *d2ssect* (https://github.com/bakeronit/d2ssect), based on D_2^S metric.[119] Samples containing similar symbiont compositions are expected to share similar *k*-mer profiles (i.e., short D_2^S-derived distance). The D_2^S-derived distance matrix was used to perform an unconstrained principal coordinate analysis (PCoA)[147] using the *cmdscale* function in R, and was used to infer a neighbour-joining tree using R package *ape* v5.8.1.[120]

To validate the aforementioned methods using a conventional amplicon-based approach, a subset of 36 DNA samples distributed across host populations were used for ITS2 marker amplification (Herculase II Fusion DNA Polymerase Nextera XT Index V2 Kit) and Illumina sequencing at Macrogen (Seoul, Korea) using forward primer SYM_VAR_5.8S 5'-GAATTGCAGAACTCCGT GAACC-3' and reverse primer SYM_VAR_REV 5'-CGGGTT CWCTTGTYTGACTTCATGC-3'.[101] ITS2 sequence data were submitted to the SymPortal analytical framework (https://symportal.org)[44] and ITS2 sequence variants and type profiles output by the pipeline were used to visualize the results. For this subset of 36 individuals, *graftM* results were checked for consistency with SymPortal results using a relative abundance barplot of ITS2 sequence variants (Figure S6A). Using the same set of samples, we also compared the hierarchical clustering of Unifrac distances based on ITS2 'defining intragenomic variants' with that based on D_2^S distances, which showed great consistency (Figure S6B) and thus we named each of the D_2^S clusters according to its corresponding major ITS2 sequence. Both dendrograms were aligned to build a tanglegram with R package *dendextend* and the stepside method.[121]

Host and symbiont co-clustering analysis

To visualize how Symbiodiniaceae communities varied across host populations, we performed a hierarchical clustering of samples using the pairwise distance matrix derived from the D_2^S metric (above) using all samples ($n = 878$) for which > 50 M bp of reads mapped to the reference Symbiodiniaceae genomes. This dendrogram was pruned to build a tanglegram with the host phylogenetic tree obtained in *RAxML* using *dendextend*.

Environmental data acquisition

To assess environmental conditions driving symbiont community composition across coral host populations and our study range, we retrieved environmental data from several satellite products and model reanalysis (Table S5). These datasets were preferred to more fine-scale resolution models available in each country for consistency reasons. We focused on variables that are known to affect Symbiodiniaceae communities structuring and can be accurately estimated in both reef systems. Temperature metrics were computed from the Coral Watch v3.1 sea surface temperature (SST) satellite product (NOAA; 1985–present; 5km).[99] Light intensity metrics (Cloud fraction and UV radiation) were computed from the ERA5 reanalysis (Copernicus marine service; 2002–present; 0.25°).[100] Water turbidity (Kd_{490nm}) and chlorophyll content metrics were computed from ESA Globcolour satellite product (2009; 2002–present; 1/24°).[148] Finally, we included spatial descriptors in the analysis such as colony-level depth and the shortest haversine distance between reefs and the coastline of Australia or New Caledonia.

QUANTIFICATION AND STATISTICAL ANALYSIS

Population statistics

A dataset of linked SNPs was used to compute population genetic differentiation and diversity estimates retaining SNPs with a minimum mean locus depth of 5 and a maximum of 50, a minimum allele count (MAC) of 1, a *p-value* of deviation from HWE test >0.0001 and < 20% missingness (“Dataset 2”, Table S4) following recommendations of Hemstrom et al.[138] To generate unbiased estimates of population genomic statistics despite missing data, the SNP dataset was concatenated to include invariant sites, filtered with the same depth and missingness thresholds per above, and used to compute statistics with *pixy* v1.2.10.[114] Following Sopniewski and Catullo,[149] 10 replicates of 5 randomly selected individuals per population were used to compute the fixation index (F_{st}) using the Weir and Cockerham method.[136] Because F_{st} estimates can be affected by within population diversity, we also computed absolute divergence (D_{xy}) for each replicate, to get more-independent estimates of population differentiation. Finally, we computed nucleotide diversity (π) within each population. We reported the median F_{st}, D_{xy} and π estimates across replicates.

Isolation by distance analysis and estimating N_e

To estimate realized dispersal and effective population sizes, Dataset 2 was further filtered to retain SNPs with <10% missing data and physically pruned to remove SNPs separated by <20 kb, retaining one SNP selected at random (“Dataset 4”). This was done because both isolation by distance (IbD) analyses and N_e estimation methods require no physical linkage.[22]

Using this dataset, we estimated σ that represents ecologically relevant gene flow averaged across the last 10–15 generations, following Prata et al.[19] with modifications. Multiple IbD regressions were performed in *spagedi* v1.5[116] using the empirical estimate of Rousset’s individual genetic distance (â)[150] and the geographic distance between individuals. Geographic distances were calculated using the Haversine formula, that estimates great-circle distances between latitude-longitude pairs. Regression analyses conducted within each of the four populations (corresponding to geographic regions; Figure 1) revealed no significant IbD. Because we were interested in a general dispersal estimate across the species range and the F_{st} estimates amongst populations were low, we used the global dataset for conducting the IbD analysis. Different regressions were performed to estimate the slope β for a range of spatial scales that roughly evenly partitioned the dataset (maximum distance of 50 m to 2,300 km). We queried multiple spatial scales in order to select *a posteriori* the appropriate regression distance spanning minimum σ and maximum 10–50 σ following Hardy and Vekemans.[151] The dimensionality of the habitat was determined for each regression by the width to area ratio, using a 1D analysis for a ratio <0.1 and a 2D analysis and the $\log_{10}$ of geographic distance for a ratio >0.1.[17] Similarly, for multiple spatial scales, the population density (D_e) was estimated by dividing the effective population size by the habitat area (A) for 2D or length (L) for 1D regressions (see below). Confidence intervals for β were estimated using a jackknifing procedure across individuals and the slope was deemed significant when the confidence intervals did not span 0. All β and D_e estimates were then combined to estimate σ at each spatial scale using the following isolation-by-distance model equation.[16,17] In the case of the 2D regression, the corresponding equation is:

$$\sigma = \sqrt[2]{\frac{1}{\beta 4\pi D_e}}$$

The linkage disequilibrium method was used to estimate the effective population size (N_e) at the neighborhood extent (radius of 2σ), which N_e represents the effective number of individuals that can easily mate in a continuously distributed population (N_b).[152] Neighborhood N_e was estimated using *LD*N_e v2.1[153] with a minimum allele frequency filter (Pcrit) based on the number of samples (S) following authors recommendations ($P_{crit} = 0.01$ if $S > 100$, $P_{crit} = 0.02$ if $S > 35$, and $1/2S < P_{crit} < 1/S$ if $S < 25$).[117] Confidence intervals were obtained for N_e using the jackknifing procedure.

Finally, we filtered our β, σ and N_e estimates to ensure that the spatial scales at which the IbD regression was performed matched a σ value ranging from σ to 10–50σ following Hardy and Vekemans.[151] We also removed any instance where N_e was not estimated at the neighborhood area, A or L equating to $4\pi\sigma^2$ for two dimensional habitat (or $2\sqrt{\pi}\sigma^2$ for one dimension) because this is the ideal spatial scale to estimate N_e.[152] Upper and lower confidence intervals for filtered estimates were then used to obtain distributions of β and N_e through resampling (n=100). A gamma distribution was used for N_e and a log-normal distribution for β. These distributions were then combined to create a joint σ distribution and propagate the error from each separate analysis.

Distance based redundancy analysis

We first investigated the influence of geography and environmental conditions on the global host population structure of *A.* cf. *spathulata* across the Western Pacific (n = 999). For this purpose, we retrieved spatial predictors (reef distance to the coast, colony-level depth), and environmental predictors from several satellite products and models with a focus on variables known to be primary drivers of coral holobiont community composition (temperature, light and turbidity; see STAR Methods, environmental data acquisition and Table S5). We modeled spatial relationships among colonies using distance-based Moran's Eigenvector Maps (dbMEMs), which capture multi-scale spatial relationships using principal coordinate analyses.[147] As individual colony-level GPS coordinates were not recorded at NC and CB reefs, randomly jittered coordinates within 300 m around the reef coordinate (recorded using a GPS during sampling; corresponding to the approximate size of the sampling area) were assigned to each colony at these reefs. The neighbor matrix for each colony was computed from spatial coordinates using Haversine distance in R package *geosphere*[122] and used to compute dbMEMs eigenvectors using R package *adespatial*.[123] The first four eigenvectors associated with positive eigenvalues were kept in further analyses based on a screeplot of cumulative variance explained (>95%). All predictors were standardized by subtracting the mean and dividing by the standard deviation to ensure comparable units.

We performed a redundancy analysis (RDA)[154] using R package *vegan*.[124] RDA is an unsupervised, constrained method (i.e., it makes no prior assumptions about the number of clusters) designed to identify axes that maximize the variance explained by a set of predictors. The first RDA model was built using the first 10 principal components of the PCA on host SNPs as a dependent matrix, and all environmental variables as predictors. Collinear predictors were removed successively, starting with the variables with the highest variance inflation factor (VIF), recomputing the model VIF and repeating this procedure until all predictors had a VIF < 10. Model significance was tested using an analysis of variance (ANOVA) and individual axes significance was tested using an ANOVA-like permutation test in package *vegan* with 500 permutations per axis. Forward selection was used to select predictors that were statistically significant. We used the framework developed by Capblancq and Forester[155] to assess the relative influence of geography and environment on host structure. We built a global RDA model using (1) environmental variables previously identified as significant using forward selection and (2) the first four dbMEM eigenvectors as predictors. Separate partial RDA models were built setting either environmental variables or spatial eigenvectors as conditional variables (i.e., 'partialled out'). Model significance was tested using an ANOVA and models were compared based on inertia, total variance explained, and proportion of constrained variance explained.

We used a similar approach to investigate the influence of geography, environmental factors and host population structure on the differentiation of *A.* cf. *spathulata* symbiont communities which are horizontally acquired.[54] Our preliminary analysis showed that ordinations based on *k*-mer-derived D_2^S distance were influenced by the number of symbiont reads in each sample. Consequently, all samples were downsampled at random to 50 M bp using *BBMap* v35.85 (*reformat.sh* script) and only samples above this threshold were retained (90% of samples, n = 878). As a small effect on the ordination remained, we included this variable as a conditional variable in all models. The first 10 principal coordinates from the PCoA on the *k*-mer D_2^S-derived distance matrix (above) were used as dependent variables in RDA models. As the PCoA did not yield negative eigenvalues indicating the distance matrix was nearly Euclidean, we did not perform negative eigenvalues correction as routinely applied in dbRDA. The first RDA model was built using all environmental variables and significant predictors were selected following the same procedure as above. A second global RDA model was built using (1) environmental variables previously identified as significant using forward selection, (2) the first four dbMEM eigenvectors and (3) the first three host PCs as predictors (representing the major axes of population structure; Figure S2E). The marginal effect of each category of predictor was then assessed through separate pRDA models, using the two other categories as conditional variables. All statistical analysis were conducted using *R* v4.0.4 and figures created using package *ggplot2*.[125]